PHYSICAL REVIEW B VOLUME 24, NUMBER 8 15 OCTOBER 1981

Diagrammatic approach to the intermediate-valence compounds

N. Grewe* and H. Keiter†
Institute for Theoretical Physics, University of California, Santa Barbara, California 93106
(Received 5 March 1981)

A model for intermediate-valence compounds is considered that is based on correlated ionic states with n_0 and n_0+1 f electrons and includes the hybridization with band electrons as a perturbation. The expansion is formulated diagrammatically with Goldstone diagrams for the strongly correlated on-site processes and Feynman propagators between different sites. Suitable infinite-order resummations of the on-site processes lead to Brillouin-Wigner-type self-consistency equations for the f quasiparticle energy shifts. The imaginary part of the single-site f-level Green's function exhibits a spike above a continuum which vanishes at the Fermi level. Deviations from the Ruderman-Kittel-Kasuya-Yosida behavior are found for the intersite terms. The effect of the shift of the chemical potential due to the fixed number of electrons is discussed.

I. INTRODUCTION

The intermediate-valence (IV) problem has remained a challenge to solid-state theoreticians ever since the earliest attempts to explain the variety of experimental data on dilute and concentrated rare-earth materials.[1] Although a considerable number of calculations have been done quite successfully,[2] a systematic treatment, which would allow—at least in principle—for estimates on the errors connected with model assumptions and/or approximations used, is still lacking.

The difficulties encountered have a twofold nature. First, it is not clear *a priori* which of the possible mechanisms of interaction is important for the explanation of any of the variety of specific experimental data. There exist, for certain, very strong Coulomb interactions among the electrons in the $4f$ shell of the rare-earth ions which have to be taken into account in the first place. Together with spin-orbit coupling and possibly the effect of the crystal field, these are responsible for the multiplet structure (which resembles that of the free ions) seen in spectroscopic experiments. Owing to the (quasi) degeneracy of two $4f$-shell configurations with an occupancy differing by one, these many-electron states become hybridized with band states ($5d$,$6s$) in the neighborhood of the Fermi level for some rare-earth ions in dilute or concentrated compounds. This is commonly regarded as the origin of the IV phenomenon. In addition to this, the residual Coulomb interactions between $4f$ and band electrons (electron-hole attraction as considered by Falicov[3]) and the coupling to the lattice degrees of freedom[4] is essential for describing the collective behavior of the compounds.

Second, the mixture of two very different kinds of electronic states, one a localized and highly correlated many-particle $4f$ state and the other belonging to extended and rather weakly interacting quasiparticles, poses certain technical difficulties. These difficulties can reveal themselves in different forms. In models such as that proposed by Anderson,[5] which simplify the orbital dynamics by using s instead of f states, the local interactions take a simple form and may be treated explicitly. However, since these interactions are very strong, they cannot be handled in mean-field theory. Introduction of a coupling to the band results in a many-body problem, which is nontrivial. Although perturbation expansions in the local interactions may be set up in the standard way, the necessary infinite-order resummations are very complicated and may prove to be insufficient as in the case of the Kondo problem.[6]

The approximate validity of an ionic level scheme, as suggested by the spectroscopic investigations, leads to a different starting point for a perturbation expansion: The local interactions are exactly included in the zero-order Hamiltonian via transfer operators between the ionic states,[7] and the hybridization with the band is treated as a perturbation. Since the transfer operators, however, do not obey simple boson- or fermion-operator rela-

tions, Wick's theorem does not hold for them, and the perturbation expansion in terms of linked Feynman diagrams is ruled out. In addition to leading to linked diagrams, the Feynman-diagram expansion of standard many-body theory has the advantage of combining $n!$ elementary excitation processes (particles and/or holes) into one nth-order diagram, and the picture of elementary processes can often be used as a guideline for approximations.

It appears then that for a perturbative treatment of the IV problem in terms of the interaction with the band, a decision has to be made from the onset: Should the terms be "linked," even if they cannot be interpreted as elementary excitation processes, or should one retain this interpretation and thereby sacrifice the linked-cluster expansion? In Hubbard's extensive studies[7,8] of the problem, the first possibility had been chosen and that was the basis for several subsequent investigations.[9–11] The "linked" terms were Kubo's generalized cumulants,[12] and the interpretation in terms of elementary excitation processes was not possible.

The main guideline for this investigation has been that all terms of the perturbation expansion have to represent elementary excitation processes, but that they should be combined into Green's functions whenever possible. This idea will be shown to lead to a mixed Feynman-Goldstone—diagram formulation in the following sense: The on-site processes are strongly correlated and have to be calculated via a finite-temperature version of Goldstone diagrams, essentially a generalization to the transfer-operator formalism of the Goldstone diagrams devised for the single-impurity Anderson model.[13] Infinite-order resummations of the on-site processes result in a Brillouin-Wigner-type scheme,[13] which has been recognized[14,15] to be well suited for dealing with the small energy denominators occurring in the IV problem. If an excitation travels via the band from one site to another, it can either be a particle or a hole, and so it is represented by a band Green's function. With this view of the processes, it is possible to obtain the many-particle Green's functions of a configuration-based model for a single impurity which may be in the IV regime, as well as many-particle Green's functions for the full multisite problem.

The basic formalism of the perturbation technique is developed in Sec. II. We encounter a new type of problem caused by the restrictions in site summations, once a specific topology of a diagram is fixed. This problem apparently has been disregarded in the literature so far. Section III deals with the mixed Feynman-Goldstone—diagram expansion and presents the complete set of rules for the corresponding analytic contributions to the partition function of a concentrated system. Section IV contains an account of the Brillouin-Wigner-type technique of performing infinite-order resummations of on-site processes with external lines and a discussion of the rules for calculating the (local) many-particle Green's functions of the single-impurity problem. It is briefly explained how the Green's functions of the concentrated system may be calculated using the same techniques. Finally, in Sec. V several applications of the formalism are discussed. In the leading logarithmic approximation the f-level single-site Green's function has an imaginary part consisting of a spike inside a gap and a continuum outside. In the next leading approximation the gap shrinks, and the spike is accompanied by a resonance on top of the continuum. The simplest intersite term shows deviations from the Ruderman-Kittel-Kasuya-Yosida (RKKY) behavior in the IV case. It is demonstrated how higher-order processes can be summed. The shift of the chemical potential due to the fixed number of electrons is shown to lead to the disappearance of the highest logarithmic singularities in the susceptibility. In leading order it also keeps the quasiparticle resonance at the Fermi level.

Of the three appendixes, the first is devoted to a definition and some rules for the ionic transfer operators. The second elaborates on the formal steps of rearrangement of the partition function and the excluded-volume-type problem encountered in Sec. II. The last Appendix gives a calculation of the perturbation series for the concentrated case up to fourth order in the mixing, thus completing previous work.[10,16]

II. BASIC PERTURBATION FORMALISM

The class of Hamiltonians to which the following perturbation technique can be applied is characterized by a perturbative part

$$H' = \sum_{\substack{\nu \vec{k} \sigma \\ M_1 M_2}} [N^{-1/2} e^{i\vec{k}\cdot\vec{R}_\nu} V_{\vec{k}}(\sigma M_1 M_2) \times d^\dagger_{\vec{k}\sigma} X^{(\nu)}_{M_1 M_2} + \text{H.c.}] = \sum_\nu H'_\nu \,, \tag{1}$$

which describes one-electron transitions between local configurations due to the mixing with band electrons, represented by creation operators $d^{\dagger}_{\vec{k}\sigma}$. In the IV case, the operator $X^{(\nu)}_{M_1M_2}$ changes a configuration of $4f$ electrons of a rare-earth ion at site ν with quantum numbers M_2 to one with quantum numbers M_1. In Appendix A some useful properties of the X operators are listed. Because of the large Coulomb repulsion between $4f$ electrons, it is usually assumed to be sufficient to include only two different $4f$ occupations, n_0 and n_0+1. The rest of the quantum numbers in M_1 and M_2 then distinguishes the various (crystal-field-split) multiplets. At low temperatures only the lowest of these contribute significantly.

The unperturbed part H_0 of the Hamiltonian $H=H_0+H'$ is assumed to be diagonal in the configurations:

$$H_0=\sum_{\vec{k}\sigma}\epsilon_{\vec{k}\sigma}d^{\dagger}_{\vec{k}\sigma}d_{\vec{k}\sigma}+\sum_{\nu,M}E_M X^{(\nu)}_{MM}$$

$$=H_{0\,\mathrm{band}}+\sum_{\nu}H_{0\nu}\,. \tag{2}$$

All energies are those of excitations with respect to the chemical potential μ and include the magnetic field splitting. Since many-body perturbation expansions are most conveniently carried out in the grand canonical ensemble, one has to keep track of the changes of μ in order to account for the electron-number conservation required in the IV situation.

One further remark seems to be in place here: In order to present the details of the formalism as clearly as possible, one should avoid very complicated diagrammatic examples as well as more "realistic" though more complicated Hamiltonians. According to this maxim, additional interactions between the electrons and (or) phonons will not be discussed here, though they can be dealt with by the same type of techniques. We shall also restrict the discussion to the partition function, keeping in mind that Green's functions can be obtained by functional derivative methods, or, from a more diagrammatical point of view, by cutting lines in the diagrams. The perturbation expansion for the partition function is set up in terms of time-ordered products of interaction operators[17]:

$$\frac{Z}{Z_0}=1+\sum_{n=1}^{\infty}\frac{(-1)^n}{n!}\int_0^{\beta}d\tau_1\cdots\int_0^{\beta}d\tau_n\langle T(H'(\tau_1)\cdots H'(\tau_n))\rangle_0$$

$$=1+\sum_{m=1}^{\infty}\frac{1}{(2m)!}\sum_{\nu_1}\int_0^{\beta}d\tau_1\cdots\sum_{\nu_{2m}}\int_0^{\beta}d\tau_{2m}\langle T(H'_{\nu_1}(\tau_1)\cdots H'_{\nu_{2m}}(\tau_{2m}))\rangle_0 \tag{3}$$

In the next step we arrange the terms according to the set of different sites involved. In $2m$th order there are $\binom{2m}{2m_1}$ possibilities for $2m_1$ interaction operators referring to site ν_1, $\binom{2m-2m_1}{2m_2}$ for $2m_2$ of the rest referring to ν_2, etc., where $2m_1,\ldots$ is any decomposition of the number $2m$ of interaction operators into non-negative integers. This results in

$$\frac{Z}{Z_0}=1+\sum_{m=1}^{\infty}\sum_{l=1}^{\infty}\sum_{\{\nu_1\cdots\nu_l\}}\sum_{\substack{m_1\cdots m_l=1\\ \sum m_j=m}}^{\infty}\left[\prod_{j=1}^{l}\frac{1}{(2m_j)!}\right]\int_0^{\beta}d\tau_1^{(1)}\cdots\int_0^{\beta}d\tau_{2m_1}^{(1)}\cdots\int_0^{\beta}d\tau_1^{(l)}\cdots\int_0^{\beta}d\tau_{2m_l}^{(l)}$$

$$\times\langle T(H'_{\nu_1}(\tau_1^{(1)})\cdots H'_{\nu_1}(\tau_{2m_1}^{(1)})\cdots H'_{\nu_l}(\tau_1^{(l)})\cdots H'_{\nu_l}(\tau_{2m_l}^{(l)}))\rangle_0$$

$$=1+\sum_{l=1}^{\infty}\sum_{\{\nu_1\cdots\nu_l\}}\sum_{m_1\cdots m_l=1}^{\infty}\int_0^{\beta}d\tau_1^{(1)}\cdots\int_0^{\tau_{2m_1}^{(1)}-1}d\tau_{2m_1}^{(1)}\cdots\int_0^{\beta}d\tau_1^{(l)}\cdots\int_0^{\tau_{2m_l}^{(l)}-1}d\tau_{2m_l}^{(l)}$$

$$\times\langle T(H'_{\nu_1}(\tau_1^{(1)})\cdots H'_{\nu_1}(\tau_{2m_1}^{(1)})\cdots H'_{\nu_l}(\tau_1^{(l)})\cdots H'_{\nu_l}(\tau_{2m_l}^{(l)}))\rangle_0\,. \tag{4}$$

In the last step we eliminated the summation restriction $\sum m_j=m$ by summing over all orders m of perturbation and the combinatorial factors $(2m_j)!$ by introducing a specific time ordering at each site (at site j, $\tau_1^{(j)}>\tau_2^{(j)}>\cdots>\tau_{2m_j}^{(j)}$).

Since H_0 is a sum of a conduction-electron part and an f-electron part at the sites, which all commute with each other, the trace with respect to H_0 over the T product in (4) factors into the corresponding contributions, in which the time sequences under the T products have to be kept:

$$\langle T(H'_{\nu_1}(\tau_1^{(1)}) \cdots H'_{\nu_l}(\tau_{2m_l}^{(l)}))\rangle_0$$
$$= \sum{}' \left[\prod_{j=1}^{l} \cdots N^{-1/2} V \cdots N^{-1/2} V^* \cdots e^{i\vec{k}\cdot\vec{R}_{\nu_j}} \cdots e^{-i\vec{k}'\cdot\vec{R}_{\nu_j}} \right.$$
$$\left. \times \langle T(\cdots X_{MM'}^{(\nu_j)}(\tau_{\cdots}^{(j)}) \cdots X_{\cdots}^{(\nu_j)}(\tau_{\cdots}^{(j)}) \cdots)\rangle_0 \right]$$
$$\times \left\langle T \left[\prod_{j=1}^{l} \cdots d_{\vec{k}\sigma}^{\dagger}(\tau_{\cdots}^{(j)}) \cdots d_{\vec{k}'\sigma'}(\tau_{\cdots}^{(j)}) \cdots \right] \right\rangle_0 . \tag{5}$$

Here, the sum extends over all possible sequences of operators at the sites and over all quantum numbers involved. It is a standard problem to find a graphical representation of (5). One simply draws a time axis and parallel to it l dotted lines, one for each site. Then one distributes dots corresponding to the interaction vertices at each site and attaches arrowed band electron lines to them (an arrow leaving the vertex stands for a creation operator). To complete the representation, the quantum numbers to be inserted (those for the f level on top and on the bottom of a site's time axis are the same). An example for two sites and six interaction times is shown in Fig. 1.

It is obvious how to assign a numerical contribution to such a "diagram" contributing to Eq. (4) or (5). In Fig. 1, for example, at time $\tau_2^{(1)}$, the dot stands for

$$N^{-1/2} \exp(-i\vec{k}_2\cdot\vec{R}_1) V_{\vec{k}_2}^{*}(\sigma_2 M_3^{(1)} M_4^{(1)}) \times X_{M_3^{(1)} M_4^{(1)}}^{(1)}(\tau_2^{(1)}) d_{\vec{k}_2\sigma_2}(\tau_2^{(1)}) .$$

At each site, a thermal average over the X operators, the sums over the quantum numbers, and the time integrals have to be evaluated. Up to this point, the contributions from the different sites involved in a term in (4) are multiplicative.

The only way to establish connections between different sites is via the thermally averaged T product over the band-electron operators in the sequence appearing in Eq. (5). Since Wick's theorem is applicable here, the average amounts to pairing the arrowed lines in the diagrams in all possible ways. Thus, the connections between the sites are established via band-electron Green's functions. At each site, however, the fixed time ordering mentioned before has to be kept in order to account for the strong on-site correlations. The absence of Wick's theorem for the X operators prevents a further evaluation of diagrams such as Fig. 1 in terms of Feynman diagrams. As will be shown in the following section, it is nevertheless possible to set up other diagrams for the contributions to Eq. (4) which can be interpreted in terms of physical processes occurring at the sites and between the sites. Finding those diagrams and their precise numerical value, however, is not the only problem: In dealing with contributions to Eq. (4), one has to face a problem which is similar to an excluded-volume problem. To see this, we imagine that the pairing of the band-electron operators has been carried out. Then different classes of terms occur. In the simplest class, the band electrons are always emitted and reabsorbed at the same site. We can graphically combine all these processes, e.g., for site j, together into a "superblock," S_j. The next

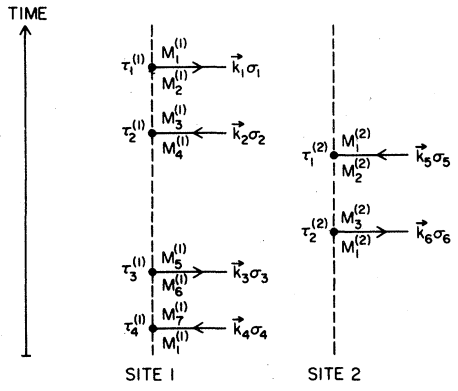

FIG. 1. Graphical representation of a sequence of interaction operators as occurring in Eqs. (4) and (5).

more complicated class of terms contains the processes in which the band electrons interact with two sites, e.g., sites i and l. For these sites a superblock S_{il} can be drawn (see Fig. 2 for an illustration). Continuing with three-site processes, etc., one finally obtains the following expansion of the partition function:

$$\frac{Z}{Z_0}=1+\sum_i S_i+\sum_{\{i,j\}}(S_iS_j+S_{ij})+\sum_{\{i,j,k\}}(S_iS_jS_k+S_{ij}S_k+S_{ik}S_j+S_iS_{jk}+S_{ijk})+\cdots . \tag{6}$$

Here, the first sum is over the single-site contributions, the second sum extends over all different pairs $\{i,j\}=\{j,i\}$, the third over all triplets, etc. To see the problem let us sum all the single-site (SS) contributions:

$$\frac{Z^{SS}}{Z_0}=1+\sum_i S_i+\sum_{i<j} S_iS_j+\sum_{i<j<k} S_iS_jS_k+\cdots=\prod_i(1+S_i)=\exp\left[\sum_i \ln(1+S_i)\right] . \tag{7}$$

Clearly the result is the exponentiated sum of the single-site free-energy corrections, as expected. Had we forgotten about the summation restrictions, the "result" would have been $\exp(\sum_i S_i)$, which is clearly invalid for $S_i \simeq 1$. Similar difficulties arise in the two-site terms, etc. They will be discussed in Appendix B.

III. THE PERTURBATION EXPANSION REPRESENTED BY MIXED FEYNMAN-GOLDSTONE DIAGRAMS

In this section we will complete the diagrammatic representation of the contributions that Eq. (4) makes to the partition function. We first may get rid of the explicit time dependence of all X operators by extracting the corresponding exponential factors in

$$X^{(\nu)}_{M_1M_2}(\tau)=e^{\tau(E_{M_1}-E_{M_2})}X_{M_1M_2} \tag{8}$$

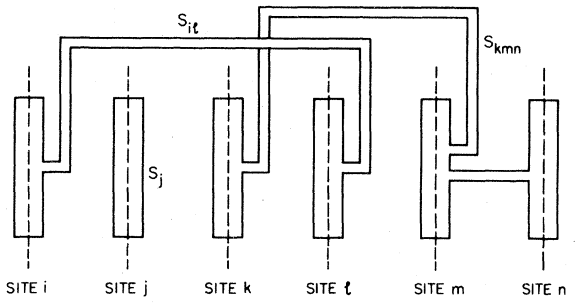

FIG. 2. Examples for superblocks.

from the expectation values.

The remaining thermal average over the X operators is simply given by [using the result (A6) from the Appendix A]

$$\langle X^{(\nu)}_{M_1M_2}X^{(\nu)}_{M_3M_4}\cdots X^{(\nu)}_{M_{2j-1}M_{2j}}\rangle_0 = P_{M_1}\delta_{M_2M_3}\cdots\delta_{M_{2j}M_1} \tag{9}$$

with the occupation probability P_{M_1} of the initial

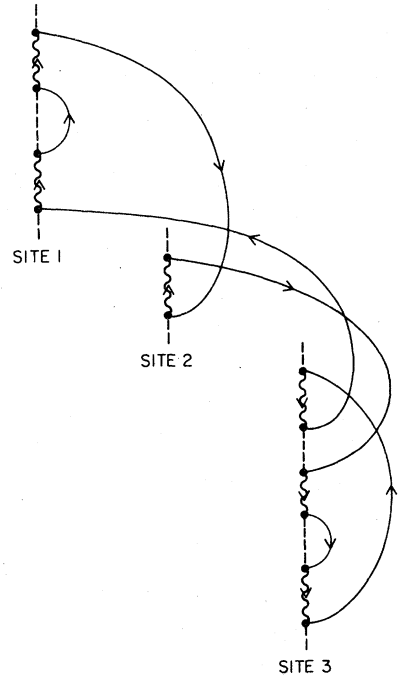

FIG. 3. Example for the decomposition of the expectation value of a time-ordered product of conduction electron operators via Wick's theorem.

state M_1 at the corresponding site,

$$P_{M_1}=e^{-\beta E_{M_1}}\left[\sum_M e^{-\beta E_M}\right]^{-1} . \tag{10}$$

Next we turn to the thermally averaged T product of d and $d^\dagger$ operators. It clearly is decomposed with the aid of Wick's theorem into a sum of products of pairings of creation and annihilation operators.[17] The pairings can be easily visualized diagrammatically. An example is shown in Fig. 3. There, the operators in (5) act from top to bottom according to the order in which they stand in the T product. The diagram contains examples for all the possible types of pairings. The first two types involve operators at the same site:

$$\langle d_{\vec{k}\sigma}(\tau_1^{(j)})d^\dagger_{\vec{k}'\sigma'}(\tau_2^{(j)})\rangle_0=\delta_{\vec{k}\vec{k}'}\delta_{\sigma\sigma'}\exp[\epsilon_{\vec{k}\sigma}(\tau_2^{(j)}-\tau_1^{(j)})](1-f_{\vec{k}\sigma}) , \tag{11}$$

$$\langle d^\dagger_{\vec{k}'\sigma'}(\tau_2^{(j)})d_{\vec{k}\sigma}(\tau_1^{(j)})\rangle_0=\delta_{\vec{k}\vec{k}'}\delta_{\sigma\sigma'}\exp[\epsilon_{\vec{k}\sigma}(\tau_2^{(j)}-\tau_1^{(j)})]f_{\vec{k}\sigma} . \tag{12}$$

Here $f_{\vec{k}\sigma}$ stands for the Fermi distribution function. The pairing (11) is represented by an ascending full wiggly line, the pairing (12) by a descending line.

The third type of pairing arises, if operators on different sites are involved:

$$\langle T(d^\dagger_{\vec{k}'\sigma'}(\tau^{(l)})d_{\vec{k}\sigma}(\tau^{(j)}))\rangle_0=-\langle T(d_{\vec{k}\sigma}(\tau^{(j)})d^\dagger_{\vec{k}'\sigma'}(\tau^{(l)}))\rangle_0$$
$$=\delta_{\vec{k}\vec{k}'}\delta_{\sigma\sigma'}G^0_{\vec{k}\sigma}(\tau^{(j)}-\tau^{(l)})=\delta_{\vec{k}\vec{k}'}\delta_{\sigma\sigma'}\frac{1}{\beta}\sum_n \exp[i\omega_n(\tau^{(j)}-\tau^{(l)})]G^0_{\vec{k}\sigma}(i\omega_n) . \tag{13}$$

In (13), the one-particle Green's function for band electrons has been introduced together with its Fourier transform[17]

$$G^0_{\vec{k}\sigma}(i\omega_n)=(i\omega_n-\epsilon_{\vec{k}\sigma})^{-1} \tag{14}$$

with $\omega_n=(2n+1)\pi/\beta$. The Green's function is represented by an arrowed intersite line. We note that in all pairings the time dependence could be split off in the form of an exponential factor.

The sign of a product of pairings (represented diagramatically as the example in Fig. 3) is read off the diagram as $(-1)^{c+b}$, where c is the total number of crossings of solid lines and b the number of solid lines going back to the left. (In Fig. 3, $b=1$ and $c=5$.) It is understood here that all solid lines enter or leave the sites at the same side and always pass a site above its latest interaction vertex. This construction corresponds precisely to the way in which one would decompose the T-product expectation value in Eq. (5) into pairings. The number b enters into the rule, because particle and holes are used for the on-site pairings, but Green's functions for the intersite ones.

As an immediate consequence of the sign rule, there is a factorization of the contributions from groups of sites which are not connected by solid lines. This allows restriction of the discussion in what follows to block-type structures being part of the "superblock" structures in Sec. II.

Returning to the example in Fig. 3, we see a specific feature of the IV problem already built in: The occupation of the $4f$ shells is either n_0 or n_0+1. If the initial state at a specific site contains n_0 electrons, only one band electron can be absorbed, and the excitation in the $4f$ shell is a particle, represented by an ascending wiggly line (see sites 1 and 2 in Fig. 3). Similarly, if the initial state contains n_0+1 electrons (see site 3 in the figure), only one electron can be emitted into the band, leaving a hole excitation behind, represented by a descending wiggly line. So an alternating sequence of emitted and absorbed band electrons at each site arises. We mention in passing that the formalism presented here can also be applied to more general situations, e.g., more occupation possibilities and multielectron excitations.

Having reduced the thermal expectation values of the $4f$ and the band electrons to simple expressions, which may finally be interpreted in terms of physical processes, the final technical step still to be performed is the integration over times. Collecting the exponential factors from (11)–(13), a general time integral at an arbitrary site has the structure

$$I=\int_0^\beta d\tau_1\int_0^{\tau_1}d\tau_2\cdots\int_0^{\tau_{n-1}}d\tau_n\exp\left[\sum_j\tau_j\Delta_j\right] , \tag{15}$$

where Δ_j is the total energy at the vertex τ_j, e.g.,

$$\Delta_j = E_{M_j} - E_{M_{j+1}} \pm \begin{bmatrix} \epsilon_{\vec{k}\sigma} \\ i\omega_m \end{bmatrix} . \tag{16}$$

The plus (minus) sign has to be chosen if the solid line leaves (enters) the vertex, and the imaginary frequencies are brought about by intersite lines entering or leaving the site under consideration. The time differences $\tau_i - \tau_{i+1} = v_i \geq 0$, $\tau_n = v_n$ are then introduced and fulfill $\sum_{i=1}^{n} v_i < \beta$. This inequality can be treated via a Laplace transform,[18] after which the integrations over the v_i can be extended to infinity and performed independently, resulting in

$$I = \frac{(-1)^n}{2\pi i} \int_{\mathscr{C}} dz\, e^{-\beta z} [(z - \mathscr{E}_0)(z - \mathscr{E}_1) \times \cdots (z - \mathscr{E}_n)]^{-1} . \tag{17}$$

Here the path $\mathscr{C}$ of integration encircles all poles in (17) in a counterclockwise direction. The $\mathscr{E}_i$ in (17) are defined by

$$\mathscr{E}_i = -\sum_{j=1}^{i} \Delta_j , \quad \mathscr{E}_0 = 0 \tag{18}$$

and can be read off from the diagrammatic part at the site by subtracting the sum of E_{M_1} and the energies of all descending solid lines from the sum of $E_{M_{i+1}}$ and the energies of all ascending solid lines appearing between the vertices at times τ_i and τ_{i+1} ($\tau_{n+1} = 0$). The intersite lines for that purpose have to be drawn to the bottom of the time axis.

We note that the algebraic sum of all the frequencies $i\omega_m$ of the intersite lines, which is precisely equal to $\mathscr{E}_n$, can be nonzero in (17), while one expects zero for corresponding processes of electronic excitations (these should reflect energy conservation because of time-translation invariance of the full problem). Indeed it is possible to achieve this goal: One has to analyze the contributions of a "family of one-site diagrams rotated on a cylinder." Such a family is drawn in Fig. 4. We denote the numerical contribution of the first member of the family symbolically by $\hat{C}_1 I_1$, where I_1 denotes the time integral and the operator $\hat{C}_1$ includes matrix elements, the Fermi factor, sign, initial occupation probability, and summations over quantum numbers. The second member of the family differs from the first in the initial occupation probability, the character of the on-site excitations, and in the excitation energies. Precisely, one has

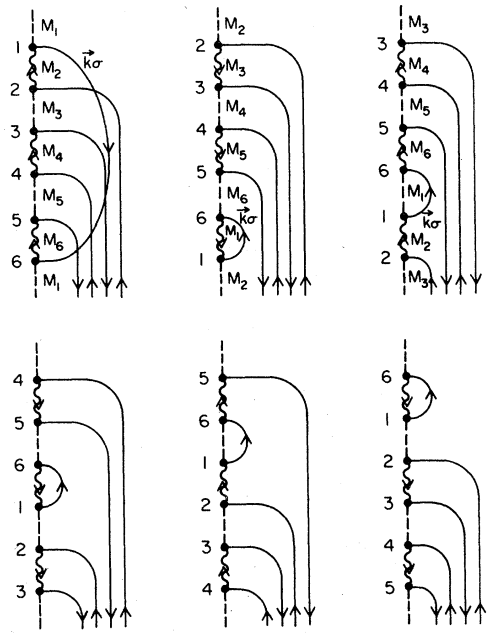

FIG. 4. Family of one-site diagrams with external lines rotated on a cylinder.

$$P_2(1 - f_{\vec{k}\sigma}) = P_1 e^{-\beta(E_{M_2} - E_{M_1})} e^{\beta\epsilon_{\vec{k}\sigma}} f_{\vec{k}\sigma} = P_1 f_{\vec{k}\sigma} e^{-\beta\mathscr{E}_1^{(1)}} ,$$
$$\mathscr{E}_i^{(2)} = \mathscr{E}_i^{(1)} - \mathscr{E}_1^{(1)}, \quad i = 2, \ldots, n-1 \tag{19}$$
$$\mathscr{E}_n^{(2)} = \mathscr{E}_n^{(1)}, \quad \mathscr{E}_0^{(2)} = \mathscr{E}_0^{(1)} = 0$$

and

$$\hat{C}_2 I_2 = \hat{C}_1 e^{-\beta\mathscr{E}_1^{(1)}} I_2 . \tag{20}$$

The result (20) is valid for the first two members of any family of rotated diagrams. We exploit the exponential factor in (20) for a shift of variables in I_2, integrating over $z + \mathscr{E}_1^{(1)}$. Proceeding with the other members of the family in the same way, the full family has a numerical contribution

$$\sum_{i=1}^{n} \hat{C}_i I_i = \hat{C}_1 \frac{(-1)^n}{2\pi i} \times \int_{\mathscr{C}} dz\, e^{-\beta z} \sum_{j=0}^{n-1} \sum_{i=j}^{n+j} (z - \mathscr{E}_i)^{-1} . \tag{21}$$

Here $\mathscr{E}_{n+l} = \mathscr{E}_n + \mathscr{E}_l$ for $l = 0, \ldots, j$.

Since $\mathscr{E}_n$ is given by the algebraic sum of an even number of frequencies $i\omega_m$, $\exp(\mathscr{E}_n) = 1$. If $\mathscr{E}_n$ is nonzero, a straightforward calculation shows that the residues at $\mathscr{E}_l$ and $\mathscr{E}_{n+l}$ cancel each other

in (21) for all l. This result is valid also if higher-order poles occur in (21). This case can be reduced to the former one by differentiation with respect to the corresponding excitation energies. Then, with $\mathscr{E}_n$ being zero, the sum in (21) may be replaced by differentiation with respect to z of the product given below, and after a partial integration one arrives at

$$\sum_{i=1}^{n} \hat{C}_i I_i = \hat{C}_1 \frac{-\beta}{2\pi i}(-1)^n \times \int_{\mathscr{C}} dz\, e^{-\beta z} \sum_{i=0}^{n-1} (z-\mathscr{E}_i)^{-1} . \quad (22)$$

Equation (22) is the final result for a family of diagrams rotated on a cylinder, if for all members the contributions are different ($\hat{C}_i I_i \neq \hat{C}_{i'} I_{i'}$ for $i \neq i'$). These diagrams are called topologically nonequivalent. The other case, in which after r rotations the family reproduces itself ($r \leq n/2$), requires a factor r/n on the right-hand side of Eq. (22). For more details, we refer to Ref. 13, where the discussion is carried out for the single-impurity Anderson model. With Eq. (22) we are in a position to state the rules for setting up and calculating the diagrams contained in a superblock with sites $\nu_1, \ldots, \nu_l$. In $2n$th order of the interaction, the rules are as follows.

(1) Draw l hatched vertical lines, one for each site, and distribute the $2n$ interaction "dots" on them in all possible ways, and at least a pair at each site. Specify the initial f-electron state at each site ν_j by a quantum number $M_l^{(j)}$. If it contains n_0 (or n_0+1) electrons, the excitation after the first, third, . . . vertex is an additional electron (hole) represented by an ascending (descending) wiggly line. Connect the vertices in all possible ways by solid arrowed lines (representing band electrons). Draw them in such a way that (a) they enter or leave the sites at the same side, (b) they pass a site on top of its uppermost interaction vertex, and (c) the direction of the arrows on wiggly and solid lines is conserved at each vertex.

(2) Assign further quantum numbers $M_i^{(j)}$ to the intermediate states of the $4f$ shell at each site, and assign momentum and spin for each band-electron line. A vertex at site ν_j with M on top of it, M' below it, and $\vec{k},\sigma$ leaving (entering) stands for $N^{-1/2} V_{\vec{k}}^{(*)}(\sigma M M') \exp[+(-)i\vec{k}\cdot\vec{R}_{\nu_j}]$. Each line contributes to the excitation energy $\mathscr{E}_i^{(j)}$ between subsequent vertices: The wiggly or dotted with quantum number $M_i^{(j)}$ contributes $E_{M_i^{(j)}} - E_{M_l^{(j)}}$; an ascending (descending) band-electron line, which does not leave site j, furnishes the energy $\epsilon_{\vec{k}\sigma}$ ($-\epsilon_{\vec{k}\sigma}$). This line furthermore contributes a statistical factor $1-f_{\vec{k}\sigma}$ (or $f_{\vec{k}\sigma}$, respectively), $f_{\vec{k}\sigma}$ being the Fermi distribution function. In order to determine the contribution of the intersite solid lines to the excitation energies at site ν_j, one should think of having them drawn to below the lowest vertex at that site. An ascending (descending) line carrying the frequency $i\omega_m$ then contributes $i\omega_m$ ($-i\omega_m$) to the excitation energy $\mathscr{E}_i^{(j)}$, if it is present between corresponding vertices. The sum over the frequencies of lines entering equals that of lines leaving the site.

(3) A solid line running between two sites and carrying $\vec{k},\sigma$ and frequency $i\omega_m$ stands for a band-electron Green's function $(1/\beta)G^0_{\vec{k}\sigma}(i\omega_m)$, as given in Eq. (14). The overall sign of the l-site diagram is given by $(-1)^{b+c}$, where c is the total number of crossings of solid lines and b the number of Green's-function lines going to the left.

(4) In $2n$th order, the numerical value $C^{2n}_{\nu_1,\ldots,\nu_l}$ of the sum of $2n$ diagrams consisting of one specified family at each site involved is obtained as follows. At each site ν_j one adds the contributions of the family of $n^{(j)}$ ($\equiv$ number of vertices) rotated diagrams. Write down a product; its factors are (a) the products of matrix elements, denoted by $\mathscr{M}^{(j)}$, (b) the initial occupation probability $P^{(j)}$, (c) the product of statistical factors, denoted by $\mathscr{S}^{(j)}$, and (d) an integral $I^{(j)}$, containing the excitation energies $\mathscr{E}_i^{(j)}$. (a)–(d) are taken for *one* (arbitrary) *representative* of the family. The integral

$$I^{(j)} = \frac{-\beta}{2\pi i}\frac{r^{(j)}}{n^{(j)}} \int_{\mathscr{C}} dz\, e^{-\beta z} \prod_{i=0}^{n^{(j)}-1} (z-\mathscr{E}_i^{(j)})^{-1} \quad (23)$$

contains the symmetry factor $r^{(j)}/n^{(j)}$ of the family, and the path $\mathscr{C}$ encircles the poles counterclockwise. Then perform the sum $\sum_{\text{intern}}^{(j)}$ over all internal quantum numbers $M^{(j)},\vec{k}^{(j)},\sigma^{(j)}$ at the site, and finally form the product of all these on-site contributions. Multiply by the intersite Green's functions, and perform the sums $\sum_{\text{inters}}$ over all intersite quantum numbers $\vec{k},\sigma;\ldots;\vec{k}',\sigma'$ as well as over all independent frequencies $i\omega_m, \ldots, i\omega_{m'}$.

The result is

$$C^{2n}_{\nu_1,\ldots,\nu_l} = \sum_{\text{inters}} \frac{1}{\beta} G^0_{\vec{k}\sigma}(i\omega_m) \cdots \frac{1}{\beta} G^0_{\vec{k}'\sigma'}(i\omega_{m'})(-1)^{b+c} \times \prod_{j=1}^{l} \sum_{\text{intern}}^{(j)} P^{(j)} \mathscr{M}^{(j)} \mathscr{S}^{(j)} I^{(j)} . \quad (24)$$

The rules so stated, for an illustration of them, representatives of the four families up to 4th order have been drawn in Fig. 5. In Appendix C, the numerical contributions are listed. Although Eq. (24) gives a compact expression for $2n$ diagrams, an easy way does not seem to exist for performing further summations of diagrams with it. To achieve this goal, one can *distribute* the contribution equation (24) of the representative diagrams *to the 2n members of the* contributing *families* of diagrams. Among the different possibilities for such distributions, there is a particularly appealing one, leading to Goldstone diagrams[19] at finite temperature. For that purpose we assign at site ν_j to the representative diagram $(1/\alpha_0^{(j)})\times$ residue of $I^{(j)}$ at $z=\mathscr{E}_0^{(j)}$ ($\alpha_0^{(j)}$ is the order of the pole at $z=\mathscr{E}_0^{(j)}$), to the first rotated family member $(1/\alpha_1^{(j)})\times$ residue of $I^{(j)}$ at $z=\mathscr{E}_1^{(j)}$, etc. As before [see Eq. (20)], the residue contributions of the rotated diagrams can be combined with the statistical factors $\mathscr{S}^{(j)}$ and the occupation probability $P^{(j)}$ to the $P^{(j)'}$ and $\mathscr{S}^{(j)'}$, which can be directly read off the rotated diagrams according to rule (2). Therefore, instead of working with the sum of $\prod_{j=1}^{l} n^{(j)}$ diagrams given in Eq. (24), one can replace rule (4) by the following:

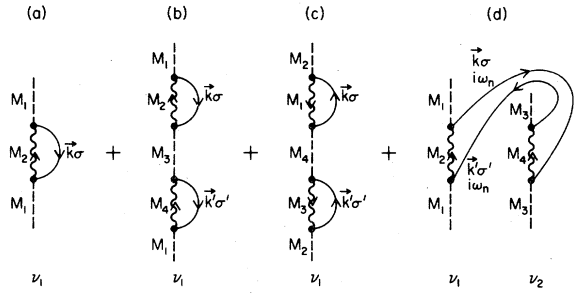

FIG. 5. Representatives of the families up to fourth order in V: (a) second-order process, (b) and (c) fourth-order on-site processes, and (d) fourth-order intersite process.

(4') The contribution of an individual diagram is given by

$$D^{2n}_{\nu_1,\ldots,\nu_l}=\sum_{\text{inters}}\frac{1}{\beta}G^{0}_{\vec{k}\sigma}(i\omega_m)\cdots\frac{1}{\beta}G^{0}_{\vec{k}'\sigma'}(i\omega_{m'})(-1)^{b+c}$$
$$\times\prod_{j=1}^{l}\sum_{\text{intern}}^{(j)}P^{(j)}\mathscr{M}^{(j)}\mathscr{S}^{(j)}(-\beta)\frac{1}{\alpha_0^{(j)}}\text{Res}_{z=\mathscr{E}_0^{(j)}=0}\left[e^{-\beta z}\prod_{i=0}^{n^{(j)}-1}(z-\mathscr{E}_i^{(j)})^{-1}\right], \tag{25}$$

where $P^{(j)}\mathscr{M}^{(j)}\mathscr{S}^{(j)}$ and $\mathscr{E}_i^{(j)}$ have to be read off the diagram as suggested in rule (2).

We note that the on-site contributions to (25) are the finite-temperature version of Goldstone diagrams, while the intersite contributions are expressed via Green's functions. The advantage of this mixed Feynman-Goldstone expansion is the built-in concept of physical processes with excitation energies and statistical factors restricting the available states. This concept is helpful for partial summations that are carried out in the next section.

IV. INFINITE-ORDER SUMMATIONS OF ON-SITE GOLDSTONE DIAGRAMS AND RELATION TO SINGLE-IMPURITY GREEN'S FUNCTIONS

As a result of the previous sections the problem has been divided into two parts: the strongly correlated on-site processes and the intersite connections by propagating band electrons. This is reflected in the structure of the diagrammatic contributions, if we assign to them numerical values according to the rules developed in the last section, especially Eqs. (24) and (25). This structure suggests the following approach: Since the intersite propagators feed into a specific site quantum numbers and frequency only, similar to time-dependent external sources, we can sum on-site processes with a given number of external lines independently. For that purpose we use generalizations of the techniques applied already to the single-site problem.[13] As is already evident from the physical picture of processes, the quantities to be calculated are essentially the on-site Green's functions.

We start from the expansion in terms of on-site Goldstone diagrams, as given in Eq. (25). Here a technical complication must be mentioned, related to the replacement of sums over wave vectors $\vec{k}$ by their continuum limit. While in the contributions of families of rotated diagrams, there are no diffi-

culties with vanishing energy denominators as may be seen from the integral equation (23), the contribution of an individual Goldstone diagram may become singular for accidentally vanishing energy denominators $(\mathscr{E}_i^{(j)})^{-1}$. Here "accidentally" means that $\mathscr{E}_i^{(j)}$ is zero only for specific values of the $\epsilon_{\vec{k}\sigma}$ contributing to it. The singularities may be avoided by a regularization procedure.[20] A physical example, in which the difficulties appear, has been reviewed by van Vleck.[21] For the problem under consideration, the same regularization procedure as that for the single-impurity Anderson model[13] can be used and will not be repeated here. It should be understood, however, that from now on the regularization of Goldstone-diagram contributions is implied, whenever necessary after performing the continuum limit.

Next we turn to partial summations of on-site diagrams. One should note here an advantage of the diagrams: These partial summations do not depend on that contribution to the sign of the multisite diagram which results from the crossings of external lines. We define a part of an on-site Goldstone diagram as linked if it does not contain excitation energies between its vertices, which are identically zero, and if the two excitation energies above and below the part are identically zero. A glance at the diagram in Fig. 5(b) then quickly reveals that this diagram consists of a product of two linked parts if $M_1=M_3$; on the other hand, if $M_1\neq M_3$, this diagram is just one linked part. To see the property of being "linked" more directly from the topology of the diagrams, we may conveniently close the dotted line to the left starting from the top and let it run into the first vertex below which there is an identically vanishing energy denominator. Then we proceed with the second linked part in the same way, etc. The dotted lines closed to the left always carry the quantum number of the initial f state. The internal quantum numbers of a linked part have to be restricted in such a way that no identically vanishing energy denominator occurs. An example is given in Fig. 6.

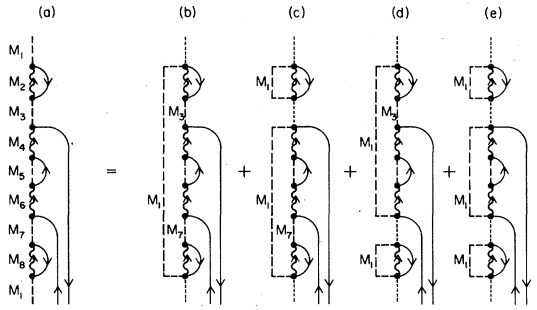

FIG. 6. Redrawing of diagram (a) with "unrestricted" internal quantum numbers into four diagrams with restricted ones: In (b) M_3 and M_7 must be different from M_1; in (c) $M_3=M_1, M_7\neq M_1$; in (d) $M_7=M_1$, $M_3\neq M_1$; in (e) $M_1=M_3=M_7$.

The matrix elements, sign factors, statistical factors, and energy denominators of the full diagram factor into those of the linked parts, as do the sums on internal quantum numbers (M_1 is kept fixed). This factorization property survives the regularization procedure. All Goldstone diagrams on site ν_j can be divided into classes according to the number $\alpha-1$ of identically vanishing energy denominators. These energy denominators separate α linked parts from each other. There are linked parts without any external lines and linked parts with an even number of external lines. We denote the sum of the numerical contributions of all linked parts at site ν_j with initial quantum number M and with κ specified external lines ($\kappa=0,2,4,\ldots$) by

$$\Gamma_M^{\kappa}(\mathscr{E}_0;\vec{k}_1\sigma_1 i\omega_1,\ \ldots\ i\omega_\kappa)\ .$$

(Of course, the algebraic sum of the external frequencies is zero.) Graphically, $\Gamma_M^{\kappa}(\cdots)$ is represented by a block with κ external lines attached to it.

The sum of contributions of all diagrams at site ν_j without external lines is just the superblock S_j. It is given by

$$S_j=-\beta\sum_{\alpha=1}^{\infty}\sum_{M}P_M\frac{1}{\alpha!}\frac{\partial^{\alpha-1}\{\exp(-\beta\mathscr{E}_0)[\Gamma_M^0(\mathscr{E}_0)]^\alpha\}}{\partial\mathscr{E}_0^{\alpha-1}}\bigg|_{\mathscr{E}_0=0}\ . \tag{26}$$

Here, the residue at $z=\mathscr{E}_0=0$ is inserted explicitly [compare Eq. (25)]. Formula (26) generalizes the result for the single-impurity Anderson model.[13] It may be cast into a more transparent shape with the aid of Lagrange's formula[22]: Let $\Phi(E)$ and $\psi(E)$ be analytic functions of E in the environment of $E=\mathscr{E}_0$, and let E be the solution of

$$E=\mathscr{E}_0+t\Phi(E) \tag{27}$$

nearest to $\mathscr{E}_0$, then $\psi(E)$ can be represented by a power series in t:

$$\psi(E)=\psi(\mathscr{E}_0)+\sum_{\alpha=1}^{\infty}\frac{t^\alpha}{\alpha!}\frac{d^{\alpha-1}\{\psi'(\mathscr{E}_0)[\Phi(\mathscr{E}_0)]^\alpha\}}{d\mathscr{E}_0^{\alpha-1}} . \tag{28}$$

Applied to Eq. (26), Lagrange's expansion yields

$$S_j+1=\sum_M P_M e^{-\beta\tilde{E}_M} \tag{29}$$

with $\tilde{E}_M$ determined from

$$\tilde{E}_M=\Gamma_M^0(\tilde{E}_M) . \tag{30}$$

Equation (30) resembles a Brillouin-Wigner expansion. The new energies $\tilde{E}_M$ are the corrections due to the change of bare particles into "statistical quasiparticles".[20]

The generalization of Eqs. (26) and (29) to the case with several linked parts ($\cong$ blocks) with a fixed sequence of specified external lines within each block is straightforward. Let there be n of those blocks at site ν_j. There are $\alpha(\alpha-1)\cdots(\alpha-n+1)$ possibilities to arrange them with respect to $\alpha-1$ energy denominators. Note that each permutation of blocks leads to an even number of additional crossings of external lines. Denoting the sum of all contributions of diagrams with those n linked parts containing the aforementioned external lines by $C_j(\cdots)$ the analog of Eq. (26) is

$$\begin{aligned}C_j(\cdots)&=-\beta\sum_{\alpha=n}^{\infty}\sum_{M_1}P_{M_1}\frac{\alpha(\alpha-1)\cdots(\alpha-n+1)}{\alpha!}\\&\quad\times\left[\frac{\partial^{\alpha-1}\{e^{-\beta\mathscr{E}_0}\Gamma_{M_1}^{\kappa_1}(\mathscr{E}_0,\ldots)\cdots\Gamma_{M_1}^{\kappa_n}(\mathscr{E}_0,\ldots)[\Gamma_{M_1}^0(\mathscr{E}_0)]^{\alpha-n}\}}{\partial\mathscr{E}_0^{\alpha-1}}\right]\Bigg|_{\mathscr{E}_0=0}\\&=-\beta\sum_{\alpha=0}^{\infty}\sum_{M_1}P_{M_1}\frac{1}{\alpha!}\left[\frac{\partial^{\alpha+n-1}\{e^{-\beta\mathscr{E}_0}\Gamma_{M_1}^{\kappa_1}(\mathscr{E}_0,\ldots)\cdots\Gamma_{M_1}^{\kappa_n}(\mathscr{E}_0,\ldots)[\Gamma_{M_1}^0(\mathscr{E}_0)]^{\alpha}\}}{\partial\mathscr{E}_0^{\alpha+n-1}}\right]\Bigg|_{\mathscr{E}_0=0} .\end{aligned} \tag{31}$$

The nth derivative with respect to $\mathscr{E}_0$ of Eq. (28) yields the formula to be used for the sum in Eq. (31):

$$\frac{\partial^n}{\partial\mathscr{E}_0^n}\psi(E)=\left[\frac{dE}{d\mathscr{E}_0}\frac{\partial}{\partial E}\right]^n\psi(E)=\left[\frac{dE}{d\mathscr{E}_0}\frac{\partial}{\partial E}\right]^{n-1}\left[\frac{dE}{d\mathscr{E}_0}\psi'(E)\right]=\sum_{\alpha=0}^{\infty}\frac{t^\alpha}{\alpha!}\frac{d^{\alpha+n-1}\{\psi'(\mathscr{E}_0)[\Phi(\mathscr{E}_0)]^\alpha\}}{d\mathscr{E}_0^{\alpha+n-1}} . \tag{32}$$

From Eq. (27) we obtain

$$\frac{dE}{d\mathscr{E}_0}=\left[1-t\frac{d\Phi(E)}{dE}\right]^{-1} . \tag{33}$$

With the aid of Eqs. (32) and (33) $C_j(\cdots)$ is expressed as

$$\begin{aligned}C_j(\cdots)=-\beta\sum_M P_M\Bigg[\left[1-\frac{d\Gamma_M^0(\tilde{E}_M)}{d\tilde{E}_M}\right]^{-1}\frac{d}{d\tilde{E}_M}\Bigg]^{n-1}\Bigg[\left[1-\frac{d\Gamma_M^0(\tilde{E}_M)}{d\tilde{E}_M}\right]^{-1}\\\times e^{-\beta\tilde{E}_M}\Gamma_M^{\kappa_1}(\tilde{E}_M,\ldots)\cdots\Gamma_M^{\kappa_n}(\tilde{E}_M,\ldots)\Bigg]\Bigg] .\end{aligned} \tag{34}$$

Here again $\tilde{E}_M$ is determined from Eq. (30).

The meaning of the factor in the parentheses may be guessed from the simple example with just one block with two external lines ($n=1,\kappa_1=2$)

$$C_j((k\sigma i\omega_n)_{\text{out}},(k'\sigma' i\omega_n)_{\text{in}})=-\beta\sum_M P_M\left[1-\frac{d\Gamma_M^0(\tilde{E}_M)}{d\tilde{E}_M}\right]^{-1}e^{-\beta\tilde{E}_M}\Gamma_M^2(\tilde{E}_M;(\vec{k}\sigma i\omega_n)_{\text{out}},(\vec{k}'\sigma' i\omega_n)_{\text{in}})\ . \tag{35}$$

Going over from bare particles to "statistical quasiparticles" requires a quasiparticle renormalization constant (Z factor), which deviates from one if the "self-energy" $\Gamma_M^0(\tilde{E}_M)$ depends on energy. Furthermore, the initial occupation probability is modified. The interpretation of the right-hand side of Eq. (35) in terms of the one-particle Green's function for the single-impurity problem, for X operators changing the occupance of the f level (M_1 and M_2' containing n_0 electrons),

$$\mathcal{F}_{M_1M_2;M_1'M_2'}(i\omega_n)=\tfrac{1}{2}\int_{-\beta}^{\beta}d\tau e^{i\omega_n\tau}\langle T(X_{M_1M_2}^{(\nu_1)}(\tau)X_{M_1'M_2'}^{(\nu_1)})\rangle_{\nu_1} \tag{36}$$

(Heisenberg picture, normalized expectation value with respect to the full $H_1=H_{0\,\text{band}}+H_{0\nu_1}+H_{\nu_1}'$ of the single-impurity problem), however, at this stage fails because of the following reasons. Firstly, the propagation of f electrons has to be calculated with a properly normalized initial occupation probability of the f level

$$\tilde{P}_M=e^{-\beta(E_M+\tilde{E}_M)}\Big/\sum_{M'}e^{-\beta(E_{M'}+\tilde{E}_{M'})}=P_M\frac{Z_0^{(1)}}{Z^{(1)}}e^{-\beta\tilde{E}_M}\ , \tag{37}$$

where $Z^{(1)}$ and $Z_0^{(1)}$ are the partition functions of the full single-impurity problem and the noninteracting one. Secondly, we have to take out the matrix elements, by which the external band electrons couple to the site and have to confine the corresponding sums to the terms with the external quantum numbers. Thirdly, in Eq. (35) only half of the processes contributing to the Green's function is contained. The other half follows from interchanging the two external lines, which acquire a minus sign from the additional crossing of external lines. Finally, the factor $(-\beta)$ has to be left out because of the definition (36) of the Green's function. Introducing blocks of diagrams for the Green's function via

$$C_j((\vec{k}\sigma i\omega_n)_{\text{out}},(\vec{k}'\sigma' i\omega_n)_{\text{in}})=-\beta\frac{Z^{(1)}}{Z_0^{(1)}}\sum_{\substack{M_1M_2\\M_1'M_2'}}e^{i(\vec{k}-\vec{k}')\cdot\vec{R}_j}V_{\vec{k}}(\sigma M_1M_2)V_{\vec{k}'}^*(\sigma' M_1'M_2')$$
$$\times\sum_M\tilde{P}_M\left[1-\frac{d\Gamma_M^0(\tilde{E}_M)}{d\tilde{E}_M}\right]^{-1}B_M^{(2)}(\tilde{E}_M;M_1M_2;M_1'M_2';i\omega_n)\ , \tag{38}$$

we finally arrive at the desired diagrammatic expansion of the single-impurity one-particle Green's function:

$$G_{M_1M_2;M_1'M_2'}(i\omega_n)=\sum_M\tilde{P}_M\left[1-\frac{d\Gamma_M^0(\tilde{E}_M)}{d\tilde{E}_M}\right]^{-1}[B_M^{(2)}(\tilde{E}_M;M_1M_2;M_1'M_2';i\omega_n)-B_M^{(2)}(\tilde{E}_M;M_1'M_2';M_1M_2;i\omega_n)] \tag{39}$$

The rules for the diagrams contributing to the B blocks follow from Eq. (38) and those of Sec. III.

One should note that the procedure of distinguishing external and internal lines, of cutting out matrix elements, etc., which led to Eq. (39), is in fact quite in the spirit of generating Green's functions from the logarithm of the partition function by functional derivatives. Diagrammatic expansion for many-particle single-impurity Green's functions can be set up along the same lines which led to Eq. (39). The topology gets more intricate, however, because the external lines can run not only into a single block, but also into several ones, and the resulting expressions, corresponding to Eq. (39) are lengthy. Perhaps the most straightforward way to visualize the resulting diagrams is the following:

One takes a pair of scissors, which acts like a differential operator, but in addition cuts lines in all possible ways, cuts out matrix elements and projects out f-level quantum numbers, furthermore replaces the cut pieces of lines by external ones, and gives a minus sign, whenever an upgoing line was cut. Denoting such an operative tool by $\hat{\mathcal{S}}(M_1M_2i\omega_n;M_1'M_2'i\omega_{n'})$, one has for the one-particle Green's function of the single-impurity problem

$$\mathcal{F}_{M_1M_2;M_1'M_2'}(i\omega_n)=-\frac{1}{\beta}\hat{\mathcal{S}}(M_1M_2i\omega_n;M_1'M_2'i\omega_{n'}) \times \ln(1+S_j)\,|_{i\omega_n=i\omega_{n'}} . \tag{40}$$

Then, applying a second pair of scissors to Eq. (40), one gets the two-particle Green's function of the one-impurity problem minus a product of two one-particle ones, bearing in mind that $1+S_j$ is $Z^{(1)}/Z_0^{(1)}$ for the single-impurity case. One then continues with the three-, four-, etc., particle Green's function.

It is clear how this scenario is generalized to the full many-site problem: Instead of $1+S_j$ in (40), one inserts the full diagrammatic expansion of the multisite partition function Z/Z_0 as outlined in Sec. III. The operative tool $\hat{\mathcal{S}}$ is kept to act on a specific site. By subsequent application of $\hat{\mathcal{S}}$, however, on different sites, one may produce two-site many-particle Green's functions, etc. It should be emphasized that this scenario leads to a diagrammatic expansion in which the contributions from the "denominator" Z/Z_0 cannot be divided out from the numerator. The on-site correlations, which prevent a Feynman-diagram expansion in the present case and lead to summations with site exclusions, also prevent a linked diagram expansion for Green's functions. To what extent resummations of diagrams nevertheless can be carried out separately for denominator and numerator follows from the first part of this section.

V. APPLICATIONS OF THE PERTURBATION TECHNIQUE

Leaving the results of finite-order perturbation technique to Appendix C, we directly turn to simple infinite order resummations of diagrams, needed for the intermediate-valence situation.

Since in finite-order perturbation calculations the most divergent terms are found in the on-site processes represented by simple buckle diagrams, such as those in Fig. 5(a)–5(c), if the diagrams there are viewed as Goldstone diagrams, we start by summing the chains of buckles. We note in passing that this approximation in fact includes all highest order divergencies. It is simple to handle if we assume an isotropic situation and the following average over the Fermi surface leading to

$$\pi\mathcal{N}_F\int\frac{d^2\Omega_{\vec{k}}}{4\pi}V_{\vec{k}}(\sigma M_0M_1)V_{\vec{k}}^{*}(\sigma M_1M_0') =\delta_{M_0M_0'}\Gamma_{\sigma M_0M_1} \tag{41}$$

($\mathcal{N}_F$ is the density of states per spin at the Fermi surface). Then the initial state is repeated after each buckle. The Γ^0's in Eq. (30) are then approximated by simple buckles [Fig. 5(a)], and Eq. (30) reads

$$\tilde{E}_{n_0N_0}=\sum_{N_1}T_{N_0N_1}(\tilde{E}_{n_0N_0}) , \tag{42a}$$

$$\tilde{E}_{n_0+1N_1}=\sum_{N_0}S_{N_0N_1}(\tilde{E}_{n_0+1N_1}) , \tag{42b}$$

where the decomposition $M_0=(n_0,N_0)$, $M_1=(n_0+1,N_1)$ has been used, and the functions T and S are given by

$$T_{N_0N_1}(z) =\frac{1}{N}\sum_{\vec{k}\sigma}|V_{\vec{k}}(\sigma M_0M_1)|^2\frac{f_{\vec{k}\sigma}}{z-E_{M_1}+E_{M_0}+\epsilon_{\vec{k}\sigma}} , \tag{43}$$

$$S_{N_0N_1}(z) =\frac{1}{N}\sum_{\vec{k}\sigma}|V_{\vec{k}}(\sigma M_0M_1)|^2\frac{1-f_{\vec{k}\sigma}}{z-E_{M_0}+E_{M_1}-\epsilon_{\vec{k}\sigma}} . \tag{44}$$

In the continuum limit, both functions develop a branch cut along the real axis and consist of two analytic pieces, holomorphic in the upper and lower half z plane, respectively. After the appropriate regularization procedure, the real part of S and T enters in Eqs. (42a) and (42b).

To be consistent with the approximation for Γ^0, one has to introduce the corresponding S and T as self-energies for the f-level Green's-function equation (39), which for zero hybridization is given by

$$\mathcal{F}_{M_0M_1;M_1',M_0'}(i\omega_n)=\delta_{M_1M_1'}\delta_{M_0M_0'}(P_{M_0}+P_{M_1}) \times(i\omega_n-E_{M_1}+E_{M_0})^{-1} . \tag{45}$$

Expressing the self-energies in terms of S and T, one obtains the following approximation for $\mathcal{F}$ [see Eq. (39)]:

$$\mathcal{F}_{M_0M_1;M_1'M_0'}(i\omega_n)=\delta_{M_1M_1'}\delta_{M_0M_0'}\left[\tilde{P}_{M_0}\left[1-\frac{d}{d\tilde{E}_{M_0}}\sum_{N_1''}T_{N_0N_1''}(\tilde{E}_{M_0})\right]^{-1}\right.$$

$$\times\left[i\omega_n-E_{M_1}+E_{M_0}+\tilde{E}_{M_0}-\sum_{N_0''}S_{N_0''N_1}(\tilde{E}_{M_0}-E_{M_1}+E_{M_0}+i\omega_n)\right]^{-1}$$

$$+\tilde{P}_{M_1}\left[1-\frac{d}{d\tilde{E}_{M_1}}\sum_{N_0''}S_{N_0''N_1}(\tilde{E}_{M_1})\right]^{-1}$$

$$\left.\times\left[i\omega_n-E_{M_1}+E_{M_0}-\tilde{E}_{M_1}+\sum_{N_1''}T_{N_0N_1''}(\tilde{E}_{M_1}-E_{M_0}+E_{M_1}-i\omega_n)\right]^{-1}\right]. \tag{46}$$

The result (46) for the single-impurity Green's function generalizes the one given in Ref. 23 for the simple three-state situation. The relation to the result of Barabanov *et al.*[9] has been established there. We note however, that the energy shifts $\tilde{E}$ are crucial for the removal of the singularities occurring in finite-order perturbation expansions. They are determined self-consistently from Eqs. (42a) and (42b). Since the functions S and T in Eqs. (43) and (44) have essentially a logarithmic structure, one can replace them by

$$\tilde{E}_{M_0}=\pi^{-1}\sum_{N_1\sigma}\Gamma_{\sigma M_0M_1}\ln(|\tilde{E}_{M_0}+E_{M_0}-E_{M_1}|/C\mathcal{N}_F)\,, \tag{47a}$$

$$\tilde{E}_{M_1}=\pi^{-1}\sum_{N_0\sigma}\Gamma_{\sigma M_0M_1}\ln(|\tilde{E}_{M_1}+E_{M_1}-E_{M_0}|/C'\mathcal{N}_F)\,. \tag{47b}$$

Here the Γ are defined in Eq. (41) and the constants C and C' are of the order of unity. For Γ independent of the quantum numbers, and in the intermediate valence situation $E_{M_0}\simeq E_{M_1}$, the sums in Eqs. (47a) and (47b) furnish essentially the degeneracy factor (equal to the number of states with n_0 or n_0+1 electrons). This degeneracy factor (present in one level only) is the essential feature of the model considered by Ramakrishnan.[15] If the degeneracy factor is large in one configuration compared to the other, Ramakrishnan's conclusion that the highest logarithmic terms are the important ones in the intermediate-valence situation is valid. If one proceeds to the stable moment regime, however, lower order divergences, reflecting the Kondo effect, have to be included self-consistently in a way suggested in Ref. 13 for the single-impurity Anderson model. Since these calculations have not been performed, we are reluctant to follow Ramakrishnan's claim[15] that the Brillouin-Wigner—type expansions break down completely in the local moment regime. It is the transition from the charge fluctuation dominated intermediate-valence region to the spin fluctuation dominated local moment region, which must be included properly in the higher-order approximations.

In the intermediate-valence regime, the energies $\tilde{E}$ are negative, as may be seen from Eqs. (47a) and (47b). We recall the fact that the difference of these quasiparticle energy renormalizations is essentially determined by the difference in the degeneracy factors. We also note that this is an essential feature in Anderson's scaling approach applied to the intermediate-valence problem.[24,25] It is not surprising that the scaling equations ob-

tained there are equivalent to the first approximation of the Brillouin-Wigner self-consistency relation, if the renormalized energy of the "local f level" is identified with the difference of the quasiparticle energies.

The fact that the self-consistently determined $\tilde{E}$ from Eqs. (47a) and (47b) are negative yields important features for the f-level Green's-function equation (46). At zero magnetic field, at zero temperature, and in the intermediate-valence situation $E_{M_1} \simeq E_{M_0}$, the imaginary parts of the functions S and T vanish for $z=\omega \pm i\delta$ approaching the real axis if $\omega<0$. Thus, in the self-energies in Eq. (46) an imaginary part on the real axis is nonzero only outside the interval $-|\tilde{E}_{M_1}|<\omega<|\tilde{E}_{M_0}|$ around the Fermi level $\omega=0$. From Eq. (42) it follows that there is precisely one pole of the f-level Green's function at $z=\tilde{E}_{M_1}-\tilde{E}_{M_0}$ on the real axis, which obviously lies inside the gap. There it represents a sharp resonance in this approximation.

For small arguments the dependence of the f-level Green's function on the degeneracy factors can be seen as follows: Replacing the sums over angular momenta by degeneracy factors and denoting by g_0 (and by g_1) the degeneracy of the states with n_0 (or n_0+1) electrons, one obtains from Eqs. (47a) and (47b)

$$g_0\tilde{E}_{M_0}=g_1\tilde{E}_{M_1}+O((\ln|\tilde{E}_{M_0}|\mathcal{N}_F)^{-1}) . \quad (48)$$

If we neglect the quasiparticle renormalization factor to the same accuracy, we have

$$\mathcal{F}_{M_0M_1;M_1'M_0'}(i\omega_n)=\delta_{M_1M_1'}\delta_{M_0M_0'}(\tilde{P}_{M_0}+\tilde{P}_{M_1}) \times\left[i\omega_n-\left[\frac{g_0}{g_1}-1\right]\tilde{E}_{M_0}\right]^{-1} . \quad (49)$$

Note that the position of the f resonance relative to the Fermi level depends on the relation of the degeneracy factors.

The highest-order logarithmic approximation clearly gives rise to two questions: (1) Is there indeed a gap for the f-level excitations, and does the resonance remain sharp? (2) Can the resonance move away from the actual chemical potential in the intermediate-valence compound?

Before discussing these two questions further, we proceed with calculating the simplest intersite processes in Fig. 5(d), using Eq. (49). As shown in Appendix C, the contribution to the partition function evaluated with $\mathcal{F}^0$ from Eq. (45) diverges as T^{-2} in the intermediate-valence situation. With $\mathcal{F}$ from Eq. (49), the contribution for the simplest f-quasiparticle intersite process is given by

$$\sum_{\{\nu_1,\nu_2\}}\tilde{C}^4_{\nu_1\nu_2}=-\frac{N}{2}\sum_{\vec{R}\neq 0}\sum_n\sum_{\substack{N_0N_1\\N_0'N_1'}}\mathcal{G}_{M_0M_1;M_1'M_0'}(\vec{R},i\omega_n)\mathcal{G}_{M_0'M_1';M_1M_0}(-\vec{R},i\omega_n)\mathcal{F}_{M_0M_1;M_1M_0}(i\omega_n) \times\mathcal{F}_{M_0'M_1';M_1'M_0'}(i\omega_n) . \quad (50)$$

Here we introduced the band Green's function, weighted by the matrix elements

$$\mathcal{G}_{M_0M_1;M_1'M_0'}(\vec{R},i\omega_n)=N^{-1}\sum_{\vec{k}\sigma}V_{\vec{k}}(\sigma M_0M_1)V^*_{\vec{k}}(\sigma M_1'M_0')\exp(i\vec{k}\cdot\vec{R})(i\omega_n-\epsilon_{\vec{k}\sigma})^{-1} \simeq -2\gamma^{M_0M_1}_{M_0'M_1'}\alpha^{-1}\exp\left[\frac{\alpha}{2}\left[-\frac{\pi}{y}|n+\tfrac{1}{2}|+i\,\mathrm{sgn}(\omega_n)\right]\right] , \quad (51)$$

and the following abbreviations have been used:

$$\alpha=2k_FR,\quad y=\beta k_F/2k_F'(\mu) , \quad (52)$$

$$\gamma^{M_0M_1}_{M_0'M_1'}=\sum_\sigma\frac{kR}{\sin kR}\int\frac{d^2\Omega_{\vec{k}}}{4\pi}V_{\vec{k}}(\sigma M_0M_1)V^*_{\vec{k}}(\sigma M_1'M_0')e^{i\vec{k}\cdot\vec{R}}\Big|_{|\vec{k}|=k_F} . \quad (53)$$

In order to obtain the last line in Eq. (51), band-structure effects have been neglected by taking into account

only the pole at $\epsilon_{\vec{k}\sigma}=i\omega_n$ in the energy integration. In the same approximation the matrix elements γ have to be taken at the Fermi surface. In contrast to Eq. (41), Eq. (53) does not furnish a simple selection rule for the M quantum numbers. In the simple case of the many-site Anderson model, discussed in Appendix C, the f-level quantum numbers on the second site are uniquely determined by those on the first site due to spin conservation. The generalization of this feature to the model under consideration, which then would provide simply a degeneracy factor for the simple intersite process, as assumed by Ramakrishnan,[15] needs further inspection, however.

With Eqs. (49), (51), and (53) inserted into Eq. (50), we obtain

$$\sum_{\{\nu_1,\nu_2\}}\tilde{C}^4_{\nu_1\nu_2}=N\beta\sum_{\vec{R}\neq 0}\left[\sum_{N_0N_1}(\tilde{P}_{M_0}+\tilde{P}_{M_1})^2\sum_{N_0'N_1'}\left|\gamma^{M_0M_1}_{M_0'M_1'}\right|^2\right]$$
$$\times\frac{\beta}{\pi^2\alpha^2}\mathrm{Re}\left[\exp\left[-\frac{\pi\alpha}{2y}+i\alpha\right]\Phi\left[\exp\left[-\frac{\pi\alpha}{y}\right],2,\tfrac{1}{2}+i\frac{\beta}{2\pi}\left[\frac{g_0}{g_1}-1\right]\tilde{E}_{M_0}\right]\right], \quad (54)$$

where Φ stands for the doubly-generalized ζ function,[26]

$$\Phi(z,s,v)=\sum_{n=0}^{\infty}(v+n)^{-s}z^n . \quad (55)$$

It has been assumed in Eq. (54) that $\tilde{E}_{M_0}=\tilde{E}_{n_0}$, $\tilde{E}_{M_1}=\tilde{E}_{n_0+1}$ in zero magnetic field.

The part in Eq. (54) following the $\vec{R}$ sum is the part of the free-energy density $\tilde{f}(R)$ due to the interaction of the two sites. Its properties are reflected in the analytic structure of Φ. Introducing $\tilde{\Delta}=(g_0/g_1-1)\tilde{E}_{n_0}$, and denoting the first set of large parentheses in Eq. (54) by γ^2, we obtain the usual RKKY behavior:

$$\tilde{f}(R)\sim\frac{y}{\beta\tilde{\Delta}^2\alpha}\gamma^2\frac{\cos\alpha}{\alpha^2}e^{-\pi\alpha/2y} \quad (56)$$

if $\alpha>>(y/\beta\tilde{\Delta})>>\alpha/\beta\tilde{\Delta}$. The exponential factor gives the temperature damping. For smaller distances ($\alpha<<y/\beta\tilde{\Delta}$), α in the prefactor $F=y/\beta\tilde{\Delta}^2\alpha$ has to be replaced by $y/\beta\tilde{\Delta}$, so $F\to\tilde{\Delta}^{-1}$, and $\cos\alpha\to\sin\alpha$; for larger distances ($\alpha>>y$) it has to be replaced there by y, so $F\to 1/\beta\tilde{\Delta}^2$.

If $\beta\tilde{\Delta}<<1$ (e.g., if there were no quasiparticle renormalization), the RKKY regime is taken over by the small distance zone. Here and in the large distance zone $\tilde{\Delta}$ has to be replaced by β^{-1}, changing $F\to\beta$ in both cases. Therefore in this situation (which, of course is the intermediate-valence situation of finite-order perturbation expansions—see Appendix C) the contribution of the simplest intersite quasiparticle process to the free energy diverges proportional to β, and the corresponding intersite interaction is of longer range than the RKKY one. The latter result agrees with Tsvelik.[27]

With a finite $\tilde{\Delta}$, the divergence is cut off at a temperature $T\sim\tilde{\Delta}$. The size of $\tilde{\Delta}$ obviously is determined by the ratio of the two degeneracy factors. Before drawing final conclusions on the importance of the intersite interactions, however, one has to examine (a) the detailed structure of γ^2, e.g., in which cases it is proportional to the degeneracy factor, as assumed in Ref. 15, (b) improved approximations for the f-level Green's function and inclusion of more complicated two-site and multisite processes, and (c) the shifting of the chemical potential, resulting from the conserved number of electrons.

While leaving problem (a) aside, and before dealing with (b) and (c), we want to briefly comment on the inclusion of more complicated intersite processes. If one sums all two-site general ladder structures indicated in Fig. 7(a), one obtains a result C of the following form (in which the single-impurity partition functions have been extracted; see Appendix B):

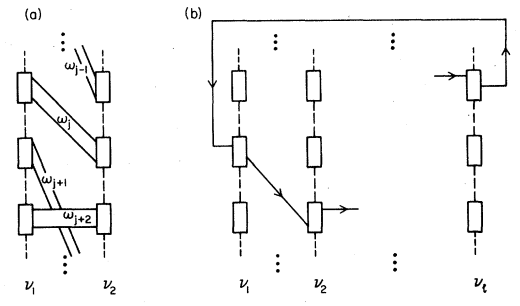

FIG. 7. (a) Two-site processes with general ladder structure; (b) many-site processes with ring structure.

$$C=\frac{N}{2}\beta^2\sum_{\vec{R}\neq 0}\sum_{m=1}^{\infty}\frac{(-1)^m}{m!}\sum_{MM'}\tilde{P}_M\tilde{P}_{M'}\hat{D}_M^{m-1}\hat{D}_{M'}^{m-1}\{z_M z_{M'}\exp(-\beta\tilde{E}_M-\beta\tilde{E}_{M'})[F_{MM'}(\tilde{E}_M,\tilde{E}_{M'})]^m\} \tag{57}$$

with

$$z_M=\left[1-\frac{d\Gamma_m^0(\tilde{E}_M)}{d\tilde{E}_M}\right]^{-1}, \tag{58}$$

$$\hat{D}_M=z_M\frac{\partial}{\partial\tilde{E}_M}, \tag{59}$$

and $[M=(n,N),\ M'=(n',N')]$

$$F_{MM'}(\tilde{E}_M,\tilde{E}_{M'})=(-1)^{n+n'}\sum_{\substack{M_1M_2M_3M_4\\M_1'M_2'M_3'M_4'}}\sum_l B_M^{(2)}(\tilde{E}_M;M_1M_2;M_3M_4;i\omega_l)\mathcal{G}_{M_1M_2;M_1'M_2'}(\vec{R},i\omega_l)$$
$$\times B_{M'}^{(2)}(\tilde{E}_{M'};M_1'M_2';M_3'M_4';i\omega_l)\mathcal{G}_{M_3'M_4';M_3M_4}(-\vec{R},i\omega_l)\ . \tag{60}$$

The blocks $B^{(2)}$ in Eq. (60) are those of Eq. (39). Because of the two differential operators, one for each site, there is no closed expression for the m sum in Eq. (57). In particular, there is no resemblance of Eq. (57) and the intersite quasiparticle energy correction given in Ref. 15, which is derived from a Brillouin-Wigner equation involving two sites. We emphasize again that the Brillouin-Wigner-type expansion used in the present paper is restricted to on-site processes.

The largest contributions to Eq. (57) at low temperatures result from the differentiation of the exponential. They can be summed to give

$$C\simeq\frac{N}{2}\sum_{\vec{R}\neq 0}\sum_{MM'}\tilde{P}_M\tilde{P}_{M'}\{\exp[-z_Mz_{M'}\beta^2F_{MM'}(\tilde{E}_M,\tilde{E}_{M'})]-1\}\ . \tag{61}$$

One should note here that the structure of the result (61) reflects the strong on-site correlations and differs markedly from a standard "disconnected" diagram summation in the partition function of the interacting electron gas, for example.

We would also like to briefly mention that simple multisite processes can be formally summed. For instance, the contribution of all the ring-type structures, Fig. 7(b), with just two band Green's functions connected to each site, to the partition function can be written as a determinant, as explicitly shown in Appendix B. This formal rearrangement of the contributions shows again that due to the excluded-site problem the algebraic structure of the partition function is more intricate than the one known from standard many-body problems. Disregarding the excluded site problem would result in destroying the strong on-site correlations. The strong on-site correlations are thus the origin of both of the difficulties discussed.

We next turn to an improved approximation for the f-level Green's function, as shown in Fig. 8. It includes the next leading logarithmic terms (compare Ref. 13). Instead of Eqs. (42a) and (42b) one obtains

$$\tilde{E}_{n_0N_0}=\Gamma_{n_0N_0}^0(\tilde{E}_{n_0N_0})=\sum_{N_1}\frac{1}{N}\sum_{\vec{k}\sigma}|V_{\vec{k}}(\sigma M_0M_1)|^2f_{\vec{k}\sigma}$$
$$\times\left[\tilde{E}_{n_0N_0}-E_{M_1}+E_{M_0}+\epsilon_{\vec{k}\sigma}-\sum_{N_0'}S_{N_0'N_1}(\tilde{E}_{n_0N_0}-E_{M_1}+E_{M_0}+\epsilon_{\vec{k}\sigma})\right]^{-1}, \tag{62a}$$

$$\tilde{E}_{n_0+1N_1}=\Gamma_{n_0+1N_1}^0(\tilde{E}_{n_0+1N_1})=\sum_{N_0}\frac{1}{N}\sum_{\vec{k}\sigma}|V_{\vec{k}}(\sigma M_0M_1)|^2(1-f_{\vec{k}\sigma})$$
$$\times\left[\tilde{E}_{n_0+1N_1}-E_{M_0}+E_{M_1}-\epsilon_{\vec{k}\sigma}-\sum_{N_1'}T_{N_0N_1'}(\tilde{E}_{n_0+1N_1}-E_{M_0}+E_{M_1}-\epsilon_{\vec{k}\sigma})\right]^{-1}. \tag{62b}$$

Repeating the discussion of Eqs. (42a) and (42b), the $\tilde{E}$ are clearly negative and again differ essentially by a degeneracy factor in the intermediate-valence situation. The approximation for the Green's function, which seems to be consistent[28] with Eqs. (62a) and (62b) is

$$\begin{aligned}\mathcal{F}_{M_0M_1;M_1M_0}(i\omega_n)=&\tilde{P}_{M_0}z_{M_0}[i\omega_n-E_{M_1}+E_{M_0}+\tilde{E}_{n_0N_0}-\Gamma^0_{n_0+1N_1}(\tilde{E}_{n_0N_0}-E_{M_1}+E_{M_0}+i\omega_n)]^{-1}\\&-\sum_{N_0'}\tilde{P}_{M_0'}z_{M_0'}\frac{1}{N}\sum_{\vec{k}\sigma}|V_{\vec{k}}(\sigma M_0'M_1)|^2 f_{\vec{k}\sigma}\Big[\tilde{E}_{n_0N_0'}-E_{M_1}+E_{M_0'}+\epsilon_{\vec{k}\sigma}\\&-\sum_{N_0''}S_{N_0''N_1}(\tilde{E}_{n_0N_0'}-E_{M_1}+E_{M_0'}+\epsilon_{\vec{k}\sigma})\Big]^{-}\\&\times\Big[\tilde{E}_{n_0N_0'}-E_{M_0}+E_{M_0'}+\epsilon_{\vec{k}\sigma}-i\omega_n\\&-\sum_{N_1'}T_{N_0N_1'}(\tilde{E}_{n_0N_0'}-E_{M_0}+E_{M_0'}+\epsilon_{\vec{k}\sigma}-i\omega_n)\Big]^{-1}+\mathcal{I}\,,\end{aligned}\tag{63}$$

where $\mathcal{I}$ represents two terms with initial occupancy n_0+1.

Discussing Eqs. (62a) (62b), and (63) as before (in zero field, low temperature, and in the intermediate-valence case), we find a reduced gap for the imaginary part of the f-level Green's function, which is determined by the difference of the quasiparticle energy corrections as calculated from Eqs. (42a) and (42b) and Eqs. (62a) and (62b). So apparently this gap is an artifact of the approximations and we expect it to close at the Fermi level in higher-order approximations. Outside of the gap the imaginary part increases, reflecting the excitations of the Fermi sea. On top of this background there is again a quasiparticle resonance, lying below the chemical potential for $g_0 > g_1$ and above it for $g_0 < g_1$. This resonance consists of a broadened part and a spike growing out of it. The spike corresponds to virtual excitations at the corresponding energy, while the width of the resonance reflects the lifetime of real excitations. Technically the origin of the broad background above the chemical potential μ comes from the first term on the right-hand side in Eq. (63) and from the last, while the background below μ comes from the other two terms. For $g_0 < g_1$ the spike results from the first term and has a large spectral weight compared to the resonance resulting from the third term.

We emphasize that there is no imaginary part of the self-energy of the first and third term in Eq. (63) at the chemical potential, and also no incoherent background (technically this results from the fact that in subsequently higher quasiparticle renormalizations the $\tilde{E}$ become more negative).

We further stress that the approximations yield one f-quasiparticle resonance. These features can be traced back in the calculations to the fact, that the $\tilde{E}$ and the self-energies have been treated on the same footing. Such a procedure is characteristic for particle-conserving approximations. The existence of a sharp resonance also prevents a simple connection between an intrinsic fluctuation temperature and a virtual level width. We do not exclude, however, that the latter may be obtained if many-site processes are taken into account.

Although part of the f resonance is sharp at low

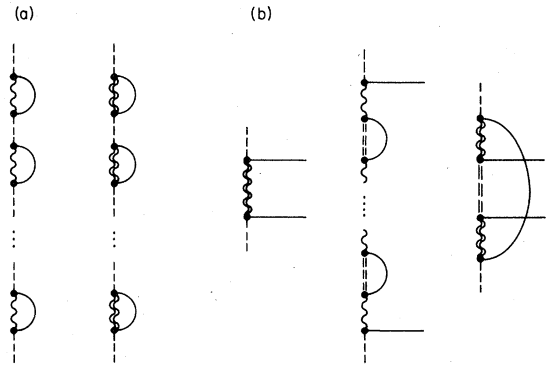

FIG. 8 Approximations including the leading [first diagrams of (a) and (b)] and next leading (other diagrams) logarithmic terms: (a) for the single-impurity partition function, (b) for a block with two external lines appearing in diagrams for the single-impurity f-electron Green's function. A double line stands for a sequence of buckles as shown in (a).

temperature, it would be naive to conclude that the zero-field magnetic susceptibility diverges. In fact, the simplest approximation, which leads to a sharp f resonance [see Eq. (46)], has been shown to give a finite susceptibility [calculated numerically[14] from the partition function equation (29) for the single-impurity problem with E taken from Eqs. (42a) and (42b)]. As already noted in Ref. 14, the decisive contribution to the susceptibility at low temperatures is

$$\chi \simeq \sum_M \tilde{P}_M \left[-\frac{\partial^2}{\partial H^2}(E_M + \tilde{E}_M) \right] , \tag{64}$$

where the sum extends over the states of the configuration with lower degeneracy. If $\tilde{E}_M$ is a smooth function of the magnetic field H at low temperatures, which is the most likely outcome of the self-consistency equation (30), the susceptibility remains finite.

For the intermediate-valence compounds, however, an important correction to the results presented so far has to be included. Since the total number $N_{\rm el}$ of electrons is conserved, the direct approach for calculating thermodynamic properties would be to use the Helmholtz free energy $F(T,N_{\rm el},H)$. The grand canonical potential $\Omega(T,\mu,H)$, which is the convenient quantity in many-body calculations, is related to F via the Legendre transform

$$F(T,N_{\rm el},H) = \Omega(T,\mu,H) + \mu N_{\rm el} , \tag{65}$$

$$N_{\rm el} = -\left. \frac{\partial \Omega}{\partial \mu} \right|_{T,H} (T,\mu,H) . \tag{66}$$

Thermodynamic quantities at fixed $N_{\rm el}$ can be calculated from Ω and its derivatives at μ_0, the chemical potential of the noninteracting system, by calculating the μ shift from Eq. (66) and by properly relating thermodynamic derivatives, e.g.,

$$\left. \frac{\partial \cdots}{\partial H} \right|_{T,N_{\rm el}} = \left. \frac{\partial \cdots}{\partial H} \right|_{T,\mu_0} + \left. \frac{\partial \mu_0}{\partial H} \right|_{T,N_{\rm el}} \left. \frac{\partial \cdots}{\partial \mu_0} \right|_{T,H} . \tag{67}$$

The correct treatment of the chemical potential can change the results of renormalized perturbation expansions quite drastically. For example, it has been shown up to V^4 that the leading logarithmic terms, resulting from on-site contributions, in the zero-field susceptibility are cancelled.[10,16] The following argument shows that this holds true in any order. Since the zero-field susceptibility as calculated from Ω in direct perturbation expansions in V contains at most corrections to the Curie law, which go like powers of $\beta \ln(\beta/\mathcal{N}_F)$, these $\ln(\beta/\mathcal{N}_F)$ powers must be contained in Ω and its derivatives with respect to μ at $\mu = \mu_0$, appearing on the right-hand side of Eq. (65). Th coupling of the magnetic field to the conduction electrons may be neglected, as it leads to corrections of the order of Zeeman energy over bandwidth for a metallic band. The prefactor in front of the logarithmic terms can be expressed as a function of the number n_f of f electrons per site. Within the same approximation, the magnetic field derivatives at fixed $N_{\rm el}$ then are those at fixed n_f. So the leading logarithmic temperature dependence of F is cancelled in its derivatives with respect to H.

As another drastic consequence of the shift of the chemical potential we discuss the position of the f-quasiparticle level with respect to the correct chemical potential. For simplicity we take the magnetic field equal to zero and characterize the intermediate-valence situation precisely by

$$E_{n_0+1} - E_{n_0} - \mu_0(0) = 0 \tag{68}$$

at $T=0$ in the noninteracting system. The number of f electrons per site is obtained from

$$\begin{aligned} n_f - n_0 = \langle X_{M_1 M_1} \rangle &= -\frac{1}{N\beta} \frac{\partial \ln Z}{\partial E_{M_1}} \\ &\simeq \sum_M \tilde{P}_M \left[\delta_{M M_1} + z_M \frac{\partial \Gamma^0_M(E_M)}{\partial E_{M_1}} \right] \\ &\simeq \tilde{P}_{M_1} = (g_1 + g_0 e^{\beta\xi})^{-1} . \end{aligned} \tag{69}$$

Equation (69) is valid to leading logarithmic order. A general value of the valence (excluding $n_f - n_0 = 0, g_1^{-1}, 1$) at $T=0$ in the interacting system can only arise, if

$$\zeta \equiv \tilde{E}_{n_0+1} - \tilde{E}_{n_0} - \delta\mu(0) = 0 . \tag{70}$$

This determines the shift $\delta\mu(0)$ of the chemical potential. If inserted in the self-consistency equations (47a) and (47b), relation (48) is again obtained. Instead of having the finite value $(g_0/g_1 - 1)\tilde{E}_{M_0}$ as in Eq. (49), the effective f-quasiparticle energy $\tilde{\Delta}$ in the denominator of the Green's function (46) vanishes to leading order. So we have $\tilde{\Delta} \sim \Gamma$ instead of $\Gamma \ln \mathcal{N}_F \Gamma$.

In this discussion only the leading logarithmic terms arising from on-site processes have been taken into account. Both the next leading terms and the intersite contributions are expected to influence

the above results quantitatively.

We conclude with a speculation as to how the shift of the chemical potential influences the result of higher-order approximations. The f-level resonance should move towards the correctly determined μ, and one might ultimately find just a spike at μ. This may result in a depletion of the density of states of the conduction electrons near μ leading to a low conductivity, similar to the effect found in recent alloy analogy calculations.[29]

ACKNOWLEDGMENTS

The authors would like to thank all members of the intermediate-valence workshop at the Institute for Theoretical Physics at UCSB for discussions and comments. This work was supported by the Deutsche Forschungsgemeinschaft (DFG) and the National Science Foundation (NSF).

APPENDIX A: PROPERTIES OF THE IONIC TRANSFER OPERATORS

In this appendix we list some properties of the ionic transfer operators $X^{(\nu)}_{M_1M_2}$ introduced by Hubbard,[7,8] which are needed in the main text. For this purpose we assume that the states of the $4f$ shell relevant for our problem are characterized by sets of quantum numbers $M \equiv (n_f, N)$, where n_f is the $4f$ occupation number and N an assembly of angular momentum and/or crystal-field level indices. For the lowest lying multiplet of a rare-earth (RE) ion for example, $N = S, L, J, J_z$, where S, L, and J are determined by Hund's rules for each particular occupation n_f, and $J_z = -J, \ldots, +J$. Any many-electron state, specified by a certain M, can be created from the $4f$ vacuum at this ion by application of a unique linear combination of products of n_f single $4f$-electron creation opertors $f^\dagger_{\nu m\sigma}$ (ν is the site index; $m = -3, -2, \ldots, 3; \sigma = \pm 1$):

$$|M\rangle_\nu = F^{(\nu)\dagger}_M |0\rangle_\nu , \tag{A1}$$

$$F^{(\nu)\dagger}_M = LC\left[\prod_{m,\sigma}^{n_f \text{ factors}} f^\dagger_{\nu m\sigma}\right] .$$

The ionic transfer operators can be defined in the following way:

$$X^{(\nu)}_{M_1M_2} = F^{(\nu)\dagger}_{M_1} P^{(\nu)}_{\text{vac}} F^{(\nu)}_{M_2} . \tag{A2}$$

Here $P^{(\nu)}_{\text{vac}}$ is the projector onto the $4f$ vacuum:

$$P^{(\nu)}_{\text{vac}} = F^{(\nu)}_{\text{tot}} F^{(\nu)\dagger}_{\text{tot}} \tag{A3}$$

where

$$F^{(\nu)\dagger}_{\text{tot}} = \prod_{m=-3}^{3} \prod_{\sigma=\pm 1} f^\dagger_{\nu m\sigma} .$$

From (A3) it is immediately clear that

$$X^{(\nu)}_{M_1M_2} |M_3\rangle_\nu = \delta_{M_2,M_3} |M_1\rangle_\nu , \tag{A4}$$

$$X^{(\nu)\dagger}_{M_1M_2} = X^{(\nu)}_{M_2M_1} , \tag{A5}$$

$$X^{(\nu)}_{M_1M_2} X^{(\nu)}_{M_3M_4} = \delta_{M_2,M_3} X^{(\nu)}_{M_1M_4} . \tag{A6}$$

The completeness relation for ionic states takes the form

$$\sum_M X^{(\nu)}_{MM} = 1 . \tag{A7}$$

In the restricted manifold of states assumed for treating the mixed valence problem, (A7) holds only approximately at low enough temperatures in an averaged sense. A thermal average over X operators gives

$$\langle X^{(\nu)}_{MM} \rangle_0 = e^{-\beta E_M}/Z_0, \quad Z_0 = \sum_{M'} e^{-\beta E_{M'}} . \tag{A8}$$

The time dependence in the interaction picture is

$$X^{(\nu)}_{M_1M_2}(\tau) \equiv e^{\tau H_{0\nu}} X^{(\nu)}_{M_1M_2} e^{-\tau H_{0\nu}} = e^{(E_{M_1} - E_{M_2})\tau} X^{(\nu)}_{M_1M_2} . \tag{A9}$$

Here an unperturbed Hamiltonian

$$H_{0\nu} = \sum_M E_M X^{(\nu)}_{MM} \tag{A10}$$

has been used. For a treatment of the many-site problem X operators on different sites have to be chosen as (anti-) commuting according to their statistical character. In general, one has

$$[X^{(\nu)}_{M_1M_2}, X^{(\mu)}_{M_3M_4}]_\pm = \delta_{\nu,\mu}(X^{(\nu)}_{M_1M_4} \delta_{M_2,M_3} \pm X^{(\nu)}_{M_3M_2} \delta_{M_1,M_4}) , \tag{A11}$$

where the $+$ sign and the anticommutor have to be used if both X are of Fermi type (Δn_f odd) and the $-$ sign and the commutator otherwise. All the above properties are simple consequences of formulas (A4) and (A6).

The Anderson model can be reformulated in the transfer operator language, as the special case of an ionic s orbital with $M = (n, \sigma)$, $n = 0, 1, 2$ and $\sigma = \pm 1$ if $n = 1$, and 0 otherwise. One readily identifies

$$X^{(\nu)}_{0,0}\equiv P^{(\nu)}_{\rm vac}=\prod_\sigma(1-n_{\nu\sigma})\quad(n_{\nu\sigma}\equiv s^\dagger_{\nu\sigma}s_{\nu\sigma})\,,$$

$$X^{(\nu)}_{1\sigma,1\sigma}=n_{\nu\sigma}(1-n_{\nu-\sigma}),\quad X^{(\nu)}_{2,2}=\prod_\sigma n_{\nu\sigma}\,,\qquad\text{(A12)}$$

$$X^{(\nu)}_{1\sigma,0}=f^\dagger_{\nu\sigma}(1-n_{\nu-\sigma}),\quad X^{(\nu)}_{2,1\sigma}=\sigma f^\dagger_{\nu-\sigma}n_{\nu\sigma}\,.$$

It is straightforward to translate the Hamiltonian from one picture to the other. For example,

$$H_{0\nu}=\sum_M E_M X^{(\nu)}_{MM}=E_0+\sum_\sigma(E_\sigma+\tfrac{1}{2}Un_{\nu-\sigma})n_{\nu\sigma}\,,$$

with (A13)

$$E_\sigma=E_{1\sigma}-E_0,\quad U=E_2+E_0-\sum_\sigma E_{1\sigma}\,.$$

In a situation appropriate to mixed valent Sm with a (nearly) degenerate $n_f=6$, $J=0$ state ($^7F_0$) and an $n_f=5$, $J=5/2$ multiplet ($^6H_{5/2}$, $J_z=5/2,-3/2,\ldots,5/2$) as lowest lying states (crystal field neglected), the Hamiltonian $H_{0\nu}$ reads

$$H_{0\nu}=E_6X^{(\nu)}_{66}+\sum_{J_z=-5/2}^{5/2}E_{5J_z}X^{(\nu)}_{5J_z,5J_z}\,.\qquad\text{(A14)}$$

Without a magnetic field the $n_f=5$ multiplet is sixfold degenerate. It is interesting to notice that such a degeneracy in both of the configurations occurs only for Th and not for Ce, Sm, Eu, and Yb.

APPENDIX B: FORMAL REARRANGEMENT OF THE PARTITION FUNCTION

The first aim of this appendix is a direct algebraical rearrangement of the partition function (4) and (5) into a form in which the superblock structure is obvious. For this purpose we start by classifying the different possibilities of connecting subsets of the l sites $\nu_1,\ldots,\nu_l$ occurring in (5) by band-electron contractions. We denote a contracted pair $d_{\vec{k}\sigma}(\tau)d^\dagger_{\vec{k}'\sigma'}(\tau')$ by the symbol c and a complete set of contractions $\{c_1,\ldots,c_m\}$ of the time-ordered expectation value of band-electron operators in (5) by $\mathscr{C}$. Let $(-1)^{\chi_{\mathscr{C}}}$ be the characteristic sign of $\mathscr{C}$ ($\chi_{\mathscr{C}}$ is the number of transpositions necessary to perform successively all contractions in $\mathscr{C}$). Since H_0 is bilinear in $d,d^\dagger$, Wicks's theorem holds and therefore

$$\left\langle T\left[\prod_{j=1}^{l}\cdots d^\dagger_{\vec{k}\sigma}(\tau^{(j)}_{\cdots})\cdots d_{\vec{k}'\sigma'}(\tau^{(j)}_{\cdots})\cdots\right]\right\rangle_0=\sum_{\mathscr{C}}(-1)^{\chi_{\mathscr{C}}}\prod_{C\in\mathscr{C}}\langle T(c)\rangle_0$$

$$=\sum_{\mathscr{P}\equiv\mathscr{P}_{\{\nu_1,\ldots,\nu_l\}}}\sum_{\mathscr{C}_{\mathscr{P}}}(-1)^{\chi_{\mathscr{C}_{\mathscr{P}}}}\prod_{C\in\mathscr{C}_{\mathscr{P}}}\langle T(c)\rangle_0\,.\qquad\text{(B1)}$$

The meaning of the new symbols introduced in the second line of (B1) is as follows: The first sum goes over all (different) partitions of the set $\{\nu_1,\ldots,\nu_l\}$ into nonempty disjunct subsets, $\mathscr{P}_{\{\nu_1,\ldots,\nu_l\}}=\{P_1,\ldots,P_p\}$, with $P_i\subset\{\nu_1,\ldots,\nu_l\}$, $P_1\cup P_2\cup\cdots\cup P_p=\{\nu_1,\ldots,\nu_l\}$, $P_i\neq\emptyset$, $P_i\cap P_j=\emptyset$. The second sum takes into account only those complete systems of contractions which establish no connections between different subsets P_i, but connect all the sites in each subset separately. These systems can obviously be written as $\mathscr{C}_{\mathscr{P}}=(C_1,\ldots,C_p)$, where C_i operates in P_i, and the sign factor can be decomposed, $(-1)^{\chi_{\mathscr{C}_{\mathscr{P}}}}=\prod_{i=1}^{p}(-1)^{\chi_{C_i}}$. With (B1) inserted into (5) and the resulting expression into (4), the following rearranged expansion is obtained:

$$\frac{Z}{Z_0}=1+\sum_{l=1}^{\infty}\sum_{\{\nu_1,\ldots,\nu_l\}}\sum_{\mathscr{P}\equiv\mathscr{P}_{\{\nu_1,\ldots,\nu_l\}}}\sum_{m_1,\ldots,m_l=1}^{\infty}\prod_{P_i\in\mathscr{P}}L_i\,.\qquad\text{(B2)}$$

The quantity

$$L_i\equiv L(P_i,(m_j/\nu_j\in P_i),C_i)$$

$$=(-1)^{\chi_{C_i}}\sum{}'\left[\prod_{\nu_j\in P_i}\cdots N^{-1/2}V\cdots N^{-1/2}V^*\cdots e^{i\vec{k}\cdot\vec{R}_{\nu_j}}\cdots e^{-i\vec{k}'\cdot\vec{R}_{\nu_j}}\cdots\right.$$

$$\left.\times\int_0^\beta d\tau_1^{(\nu_j)}\cdots\int_0^{\tau_{2m_j-1}^{(\nu_j)}}d\tau_{2m_j}^{(\nu_j)}\langle T(\cdots X^{(\nu_j)}_{\cdots}(\tau^{(\nu_j)}_{\cdots})\cdots X^{(\nu_j)}(\tau^{(\nu_j)}_{\cdots})\cdots)\rangle_0\right]\prod_{c\in C_i}\langle T(c)\rangle_0$$

(B3)

incorporates all processes of $(\sum_{\nu_j \in P_i} 2m_j)$-th order which connect all the sites in P_i. By summing all orders these can be collected into a superblock

$$S_i \equiv S(P_i) = \sum_{m_{j_1},\ldots,m_{j_\lambda}=1}^{\infty} \sum_{C_i} L(P_i,(m_{j_1},\ldots,m_{j_\lambda}),C_i) , \tag{B4}$$

which contains now all processes which take place between and actually connect the sites of P_i to a cluster. The final result then is

$$\frac{Z}{Z_0} = 1 + \sum_{\mathcal{M}\subset\mathcal{N}} \sum_{\mathcal{P}_\mathcal{M}} \prod_{\mathcal{P}\in\mathcal{P}_\mathcal{M}} S(P) , \tag{B5}$$

where $\mathcal{N}$ denotes the set of all sites. This expression is equivalent to formula (6), in which the terms of (B5) have been ordered according to the magnitude of the superblocks involved.

The problem now is to rearrange the partition function expansion equation (B5) to an exponential structure needed for the free energy. The difficulties encountered come from the exclusions in the summations on sites in Eq. (B5). Similar difficulties occur in other fields, e.g., in multiple scattering theory, in concentrated impurity systems, and for the hard-core gas. They can be attacked quite generally with cumulant expansions, of which, e.g., the Ursell-Mayer expansion is a special case which may be used for this problem. These expansions are formal, however, and can be rearranged in many ways[12] into cluster cumulants. In principle, the rearrangements should improve the convergence and also should reflect the physical intuition one has developed for the problem.

In the present problem, the single-site contributions are of particular importance, so they should be singled out in the first place. Indeed, from Eq. (B5), we immediately get

$$\frac{Z}{Z_0} = \left[\prod_{\nu\in\mathcal{N}} [1+S(\{\nu\})]\right] \times \left[1 + \sum_{\mathcal{M}\subset\mathcal{N}} \sum_{\mathcal{P}^{(2)}_\mathcal{M}} \prod_{P\in\mathcal{P}^{(2)}_\mathcal{M}} \tilde{S}(P)\right] , \tag{B6}$$

where $\mathcal{P}^{(2)}_\mathcal{M}$ contains only partitions of $\mathcal{M}$ using subsets with at least two sites. The quantity $\tilde{S}(P)$ is given by

$$\tilde{S}(P) = \frac{S(P)}{\prod_{\nu\in P}[1+S(\{\nu\})]} . \tag{B7}$$

To proceed further, one has to decide whether higher-order two-site processes are important and should be included. Without any detailed knowledge about the numerical contribution and the structure of the superblocks, however, the obvious procedure would be to try to factor out the two-site superblocks from Eq. (B6), etc. But this cannot be performed in the same way as before, since there is no unique decomposition of any given set of sites into subsets with two elements. On the other hand, the possibility of summing intersite processes of a sufficiently simple structure remains. In particular, the chain structures of Fig. 7(b) give rise to a determinant structure in the partition function. The contribution of a chain, in which the sites $\nu_1, \ldots, \nu_l$ are linked consecutively, is

$$C = -\sum_{\substack{N_0^1 N_1^1 \\ \cdots \\ N_0^l N_1^l}} \sum_p \prod_{j=1}^{l} [-\mathcal{F}_{M_0^j M_1^j; M_1^j M_0^j}(i\omega_p) \times \mathcal{G}_{M_0^j M_1^j; M_1^{j+1} M_0^{j+1}} \times (\vec{\mathrm{R}}_{j+1} - \vec{\mathrm{R}}_j; i\omega_p)] \tag{B8}$$

(where $l+1 \cong 1$ and $M_0 = n_0 N_0$, $M_1 = n_0 + 1 N_1$). The corresponding contribution for the partition function, including products of chains with any number of sites and any sequential order can be written with the aid of two matrices $\underline{\delta}$ and $\underline{k}$,

$$(\underline{\delta})_{nm} = \delta_{\omega_{p_n}\omega_{p_m}} \delta_{nm} , \tag{B9}$$

$$(\underline{k})_{nm} = \mathcal{F}_{M_0^n M_1^n; M_1^n M_0^n}(i\omega_{p_n}) \times \mathcal{G}_{M_0^n M_1^n; M_1^m M_0^m}(\vec{\mathrm{R}}_m - \vec{\mathrm{R}}_n; i\omega_{p_n}) \delta_{\omega_{p_n}\omega_{p_m}} , \tag{B10}$$

in the following way:

$$\frac{Z}{Z_0 \prod_{\nu\in\mathcal{N}} [1+S(\{\nu\})]} = \sum_{\{N_0^n, N_1^n\}} \sum_{\{p_n\}} \mathrm{Det}(\underline{\delta} + \underline{k}) . \tag{B11}$$

From Eq. (B11) one may realize the intricacy of the excluded-site problem.

APPENDIX C: SECOND- AND FOURTH-ORDER CONTRIBUTIONS TO THE PARTITION FUNCTION

First we list the contributions of the diagrams displayed in Fig. 5 according to rules (1)–(4) of Sec. III using a convenient decomposition of the sets M_i of quantum numbers:

$$M_i=(n_f=n_0,N_i)\quad (i=1,3),\quad M_j=(n_f=n_0+1,N_j)\quad (j=2,4)\,, \tag{C1}$$

$$C^{(2)}_{\nu_1}(a)=\sum_{N_1N_2}\frac{e^{-\beta E_{M_1}}}{Z_0}\frac{1}{N}\sum_{\vec{k}\sigma}f_{\vec{k}\sigma}\,|\,V_{\vec{k}}(\sigma M_1M_2)\,|^2\frac{-\beta}{2\pi i}\int_{\mathscr{C}}dz\frac{e^{-\beta z}}{z(z-E_{M_2}+E_{M_1}+\epsilon_{\vec{k}\sigma})}\,, \tag{C2}$$

$$C^{(4)}_{\nu_1}(b)=\tfrac{1}{2}\sum_{\substack{N_1,N_2\\N_3,N_4}}\frac{e^{-\beta E_{M_1}}}{Z_0}\frac{1}{N^2}\sum_{\vec{k},\sigma}\sum_{\vec{k}',\sigma'}f_{\vec{k}\sigma}f_{\vec{k}'\sigma'}V_{\vec{k}}(\sigma M_1M_2)V^*_{\vec{k}}(\sigma M_2M_3)V_{\vec{k}'}(\sigma' M_3M_4)V_{\vec{k}'}(\sigma' M_4M_1)$$

$$\times\frac{-\beta}{2\pi i}\int_{\mathscr{C}}dz\frac{e^{-\beta z}}{z(z-E_{M_2}+E_{M_1}+\epsilon_{\vec{k}\sigma})(z-E_{M_3}+E_{M_1})(z-E_{M_4}+E_{M_1}+\epsilon_{\vec{k}'\sigma'})}\,, \tag{C3}$$

$$C^{(4)}_{\nu_1}(c)=\tfrac{1}{2}\sum_{\substack{N_1,N_2\\N_3,N_4}}\frac{e^{-\beta E_{M_2}}}{Z_0}\frac{1}{N^2}\sum_{\vec{k},\sigma}\sum_{\vec{k}',\sigma'}(1-f_{\vec{k}\sigma})(1-f_{\vec{k}'\sigma'})V^*_{\vec{k}}(\sigma M_2M_1)V_{\vec{k}}(\sigma M_1M_4)V^*_{\vec{k}'}(\sigma' M_4M_3)V_{\vec{k}'}(\sigma' M_3M_2)$$

$$\times\frac{-\beta}{2\pi i}\int_{\mathscr{C}}dz\frac{e^{-\beta z}}{z(z-E_{M_1}+E_{M_2}-\epsilon_{\vec{k}\sigma})(z-E_{M_4}+E_{M_2})(z-E_{M_3}+E_{M_2}-\epsilon_{\vec{k}'\sigma'})}\,, \tag{C4}$$

$$C^{(4)}_{\nu_1\nu_2}(d)=\frac{1}{N^2}\sum_{\vec{k},\sigma}\sum_{\vec{k}',\sigma'}\frac{1}{\beta^2}\sum_n\frac{1}{i\omega_n-\epsilon_{\vec{k}\sigma}}\frac{1}{i\omega_n-\epsilon_{\vec{k}'\sigma'}}(-1)e^{i(\vec{k}-\vec{k}')\cdot(\vec{R}_{\nu_1}-\vec{R}_{\nu_2})}$$

$$\times\sum_{N_1,N_2}\frac{e^{-\beta E_{M_1}}}{Z_0}V_{\vec{k}}(\sigma M_1M_2)V^*_{\vec{k}'}(\sigma' M_2M_1)$$

$$\times\frac{-\beta}{2\pi i}\int_{\mathscr{C}}dz\frac{e^{-\beta z}}{z(z-E_{M_2}+E_{M_1}+i\omega_n)}$$

$$\times\sum_{N_3,N_4}\frac{e^{-\beta E_{M_3}}}{Z_0}V^*_{\vec{k}}(\sigma M_4M_3)V_{\vec{k}'}(\sigma' M_3M_4)$$

$$\times\frac{-\beta}{2\pi i}\int_{\mathscr{C}}dz\frac{e^{-\beta z}}{z(z-E_{M_4}+E_{M_3}+i\omega_n)}\,. \tag{C5}$$

In the following we consider the special case $J(n_f=n_0)=\frac{1}{2}$, $J(n_f=n_0+1)=0$, $V_{\vec{k}}(\sigma M_1M_2)=V_{\vec{k}}\delta_{\sigma/2,-M_1}$ (Anderson model with $n_f=1,2$ and $U\to\infty$), in which the above expressions simplify considerably:

$$C^{(2)}_{\nu_1}(a)=\sum_{\sigma}\frac{e^{-\beta E_{-\sigma}}}{Z_0}\frac{-\beta}{2\pi i}\int_{\mathscr{C}}dz\frac{e^{-\beta z}}{z}T_\sigma(z)\,, \tag{C6}$$

$$C^{(4)}_{\nu_1}(b)=\tfrac{1}{2}\sum_{\sigma}\frac{e^{-\beta E_{-\sigma}}}{Z_0}\frac{-\beta}{2\pi i}\int_{\mathscr{C}}dz\frac{e^{-\beta z}}{z^2}[T_\sigma(z)]^2\,, \tag{C7}$$

$$C_{\nu_1}^{(4)}(c)=\frac{1}{2}\frac{e^{-\beta E_2}}{Z_0}\frac{-\beta}{2\pi i}\int_{\mathscr{C}}dz\frac{e^{-\beta z}}{z^2}\left[\sum_\sigma S_\sigma(z)\right]^2, \tag{C8}$$

$$C_{\nu_1\nu_2}^{(4)}(d)=-\sum_\sigma\sum_n\left[\frac{e^{-\beta E_{-\sigma}}}{Z_0}\mathscr{G}_\sigma(\Delta\vec{\mathrm{R}}_{12};i\omega_n)\frac{1}{2\pi i}\int_{\mathscr{C}}dz\frac{e^{-\beta z}}{z(z-\Delta_{-\sigma}+i\omega_n)}\right]^2. \tag{C9}$$

Here E_σ and E_2 are the energies of the singly and doubly occupied local level, $\Delta_\sigma \equiv E_2 - E_\sigma$, and

$$T_\sigma(z)=\frac{1}{N}\sum_{\vec{k}}|V_{\vec{k}}|^2\frac{f_{\vec{k}\sigma}}{z+\epsilon_{\vec{k}\sigma}-\Delta_{-\sigma}}, \tag{C10}$$

$$S_\sigma(z)=\frac{1}{N}\sum_{\vec{k}}|V_{\vec{k}}|^2\frac{1-f_{\vec{k}\sigma}}{z-\epsilon_{\vec{k}\sigma}+\Delta_{-\sigma}}, \tag{C11}$$

$$\mathscr{G}_\sigma(\Delta\vec{\mathrm{R}}_{12};i\omega_n)=\frac{1}{N}\sum_{\vec{k}}|V_{\vec{k}}|^2\frac{e^{i\vec{k}\cdot(\vec{\mathrm{R}}_{\nu_1}-\vec{\mathrm{R}}_{\nu_2})}}{i\omega_n-\epsilon_{\vec{k}\sigma}}. \tag{C12}$$

The single-site contributions (C6)—(C8) are evaluated by residue techniques with the result

$$C_{\nu_1}^{(2)}(a)=-\sum_\sigma P_{-\sigma}\beta[T_\sigma(0)+e^{-\beta\Delta_{-\sigma}}S_\sigma(0)], \tag{C13}$$

$$C_{\nu_1}^{(4)}(b)=-\sum_\sigma\tfrac{1}{2}P_{-\sigma}\beta\left[\frac{\partial}{\partial x}\{e^{-\beta x}[T_\sigma(x)]^2\}_{x=0}+2e^{-\beta\Delta_{-\sigma}}\frac{1}{N^2}\sum_{\vec{k}\vec{k}'}|V_{\vec{k}}|^2|V_{\vec{k}'}|^2\times\frac{1-f_{\vec{k}\sigma}}{(\epsilon_{\vec{k}\sigma}-\Delta_{-\sigma})^2}\frac{f_{\vec{k}'\sigma}}{\epsilon_{\vec{k}\sigma}-\epsilon_{\vec{k}'\sigma'}}\right], \tag{C14}$$

$$C_{\nu_1}^{(4)}(c)=-\tfrac{1}{2}P_2\beta\left\{\frac{\partial}{\partial x}\left[e^{-\beta x}\left[\sum_\sigma S_\sigma(x)\right]^2\right]_{x=0}+2\sum_\sigma e^{-\beta\Delta_{-\sigma}}\frac{1}{N^2}\sum_{\vec{k}\vec{k}'\sigma'}|V_{\vec{k}}|^2|V_{\vec{k}'}|^2\frac{f_{\vec{k}}}{(\epsilon_{\vec{k}\sigma}-\Delta_{-\sigma})^2}\frac{1-f_{\vec{k}'\sigma'}}{\epsilon_{\vec{k}\sigma}-\epsilon_{\vec{k}'\sigma'}-\Delta_\sigma+\Delta_{\sigma'}}\right\}, \tag{C15}$$

$$C_{\nu_1\nu_2}^{(4)}(d)=-P_2^2\sum_{\sigma,n}(1+e^{\beta\Delta_{-\sigma}})^2[\mathscr{G}_\sigma(\Delta\vec{\mathrm{R}}_{12};i\omega_n)(\Delta_{-\sigma}-i\omega_n)^{-1}]^2$$

$$=2\beta P_2^2\sum_\sigma(1+e^{\beta\Delta_{-\sigma}})^2\beta\left[\frac{\Gamma}{\pi\alpha}\right]^2\mathrm{Re}\left[\exp\left[\frac{-\alpha\pi}{2y}+i\alpha\right]\Phi\left[\exp\left[\frac{-\pi\alpha}{y}\right],2,\tfrac{1}{2}+\frac{i\beta\Delta_{-\sigma}}{2\pi}\right]\right]. \tag{C16}$$

Equation (C16) is a special case of Eqs. (50) and (54) (without the summations over the sites). The quantities α, y, Φ are defined there and $\Gamma = \pi\mathscr{N}_F\langle|V_{\vec{k}}|^2\rangle_{\mathrm{av}}$. In the intermediate valence case $\beta\Delta \ll 1$ one has $\Phi \to (\frac{3}{2})^{-2}$ and clearly the contribution diverges proportional to β^2. For $\beta\Delta \gg 1$, however, $\Phi \sim \beta^{-1}$ and the contribution diverges only proportional to β, so the free-energy contribution is finite. The divergencies of the other terms can be easily seen if one realizes that the real part of $S_\sigma(z)$ and $T_\sigma(z)$ from Eqs. (C10) and (C11) diverges logarithmically in T, H, or Δ, whatever is the largest of these quantities, if they become small. So in the intermediate-valence case the second-order contribution diverges as $\beta\ln(\mathscr{N}_F\max\{H,T\})$, and the fourth-order contribution has a quadratic divergence in this quantity, coming from the x derivative of the exponential. The sums over $\vec{k}$ and $\vec{k}'$ contain one logarithm less in their leading divergence.

*On leave of absence from Institut für Theoretische Physik, Universität Köln, D-5000 Köln 41, Federal Republic of Germany.
†Permanent address: Physics Department, Universität Dortmund, D-4600 Dortmund 50, Federal Republic of Germany.

[1]D. K. Wohlleben and B. R. Coles, in *Magnetism V,* edited by H. Suhl (Academic, New York, 1973).
[2]For recent reviews see J. M. Jefferson and K. W. Stevens, J. Phys. C 11, 3919 (1978); N. Grewe, H. J. Leder, and P. Entel, in *Festkörperprobleme XX,* edited by J. Treusch (Vieweg, Braunschweig, 1980).
[3]R. Ramirez, L. M. Falicov, and J. C. Kimball, Phys. Rev. B 2, 3383 (1970).
[4]L. L. Hirst, J. Phys. Chem. Solids 35, 1285 (1975); N. Grewe and P. Entel, Z. Phys. B 33, 331 (1979).
[5]P. W. Anderson, Phys. Rev. 124, 41 (1961).
[6]K. G. Wilson, Rev. Mod. Phys. 47, 773 (1975); P. Nozières, *Proceedings of the 14th International Conference on Low Temperature Physics,* (North-Holland, Amsterdam, 1974), Vol. V, p. 339.
[7]J. Hubbard, Proc. R. Soc. London, Ser. A 277, 237 (1964).
[8]J. Hubbard, Proc. R. Soc. London, Ser. A 296, 82 (1967).
[9]A. F. Barabanov, K. A. Kikoin, and L. A. Maksimov, Teor. Mat. Fiz. 20, 364 (1974); 25, 87 (1975).
[10]A. C. Hewson, J. Phys. C 10, 4973 (1977).
[11]Y. Kuramoto, Z. Phys. B (in press).
[12]R. Kubo, J. Phys. Soc. Jpn. 17, 1100 (1962).
[13]H. Keiter and J. C. Kimball, Int. J. Magn. 1, 233 (1971); J. Appl. Phys. 42, 1460 (1971).
[14]A. Bringer and H. Lustfeld, Z. Phys. B 22, 213 (1977); H. Lustfeld and A. Bringer, Solid State Commun. 28, 119 (1978).
[15]T. V. Ramakrishnan, in *Proceedings of the International Conference on Valence Fluctuations in Solids, Santa Barbara, 1981,* edited by L. Falicov, W. Hanke, and M. B. Maple (North-Holland, Amsterdam, 1981).
[16]T.-K. Lee and S. Chakravarty, Phys. Rev. B 22, 3609 (1980).
[17]See, for example, A. L. Fetter and J. D. Walecka, *Quantum Theory of Many-Particle Systems* (McGraw-Hill, New York, 1971).
[18]C. Bloch, in *Studies in Statistical Mechanics,* edited by J. de Boer and G. E. Uhlenbeck (North-Holland, Amsterdam, 1965), Vol. III, Chap. 14.1.
[19]J. Goldstone, Proc. R. Soc. London, Ser. A 239, 267 (1957).
[20]R. Balian and C. de Dominicis, Ann. Phys. (N.Y.) 62, 229 (1971).
[21]J. H. van Vleck, Rev. Mod. Phys. 34, 681 (1962).
[22]E. T. Whittaker and G. N. Watson, *A Course of Modern Analysis,* 4th ed. (Cambridge University Press, Cambridge, 1978), p. 132 ff.
[23]H. Keiter and N. Grewe, in *Proceedings of the International Conference on Valence Fluctuations in Solids, Santa Barbara, 1981,* Ref. 15.
[24]J. H. Jefferson, J. Phys. C 10, 3589 (1977).
[25]F. D. M. Haldane, Phys. Rev. Lett. 40, 416 (1978).
[26]*Higher Transcendental Functions,* edited by A. Erdélyi (McGraw-Hill, New York, 1953), Vol. I, p. 27.
[27]A. M. Tsvelik, Zh. Eksp. Teor. Fiz. 76, 2260 (1979) [Sov. Phys.—JETP 49, 1142 (1979)].
[28]A formal proof for conserving approximations [see G. Baym, Phys. Rev. 127, 1391 (1962)] within the Brillouin-Wigner-type expansion apparently has not been given.
[29]See the contributions of H. J. Leder and G. Czycholl, in *Proceedings of the International Conference on Valence Fluctuations in Solids, Santa Barbara, 1981,* Ref. 15.